Geobiology

Geobiology (2012), **10**, 130–149 DOI: 10.1111/j.1472-4669.2011.00303.x

Chemical and structural status of copper associated with oxygenic and anoxygenic phototrophs and heterotrophs: possible evolutionary consequences

O. S. POKROVSKY,[1] G. S. POKROVSKI,[1] L. S. SHIROKOVA,[1,2] A. G. GONZALEZ,[3] E. E. EMNOVA[4] AND A. FEURTET-MAZEL[5]

[1]*Géosciences Environnement Toulouse (GET), UMR 5563 CNRS, Université de Toulouse, Toulouse, France*
[2]*Institute of Ecological Problems of the North, Russian Academy of Science, Arkhangelsk, Russia*
[3]*Departamento de Química, Facultad de Ciencias del Mar, Universidad de Las Palmas de Gran Canaria, Las Palmas, Spain*
[4]*Institute of Genetics and Plant Physiology, Moldavian Academy of Science, Chisinau, Moldova*
[5]*Université de Bordeaux 1, CNRS, UMR 5805 EPOC, Arcachon, France*

ABSTRACT

Copper adsorption on the surface and intracellular uptake inside the cells of four representative taxons of soil and aquatic micro-organisms: aerobic rhizospheric heterotrophs (*Pseudomonas aureofaciens*), anoxygenic (*Rhodovulum steppense*) and oxygenic (cyanobacteria *Gloeocapsa* sp. and freshwater diatoms *Navicula minima*) phototrophs were studied in a wide range of pH, copper concentration, and time of exposure. Chemical status of adsorbed and assimilated Cu was investigated using *in situ* X-ray absorption spectroscopy. In case of adsorbed copper, XANES spectra demonstrated significant fractions of Cu(I) likely in the form of tri-coordinate complexes with O/N and/or S ligands. Upon short-term reversible adsorption at all four studied micro-organisms' cell surface, Cu(II) is coordinated by 4.0 ± 0.5 planar oxygens at an average distance of 1.97 ± 0.02 Å, which is tentatively assigned to the carboxylate groups. The atomic environment of copper incorporated into diatoms and cyanobacteria during long-term growth is similar to that of the adsorbed metal with slightly shorter distances to the first O/N neighbor (1.95 Å). In contrast to the common view of Cu status in phototrophic micro-organisms, XAFS failed to detect sulfur in the nearest atomic environment of Cu assimilated by freshwater plankton (cyanobacteria) and periphyton (diatoms). The appearance of S in Cu 1st coordination shell at 2.27–2.32 Å was revealed only after long-term interaction of Cu with anoxygenic phototrophs (and Cu uptake by soil heterotrophs), suggesting Cu scavenging in the form of sulfhydryl, histidine/carboxyl or a mixture of carboxylate and sulfhydryl complexes. These new structural constraints suggest that adsorbed Cu(II) is partially reduced to Cu(I) already at the cell surface, where as intracellular Cu uptake and storage occur in the form of both Cu(I)-S linked proteins and Cu(II) carboxylates. Obtained results allow to better understand how, in the course of biological evolution, micro-organisms elaborated various mechanisms of Cu uptake and storage, from passive adsorption and uptake to active, protein-controlled surface reduction, and intracellular storage.

Received 10 June 2011; accepted 29 September 2011

Corresponding author: O. S. Pokrovsky. Tel.: +33 5 61 33 26 25; fax: +33 5 61 33 25 60; e-mail: oleg@get.obs-mip.fr

INTRODUCTION

Compared with other essential oligoelements, copper is particularly interesting as it combines versatile chemical behavior and coordination chemistry with multiple oxidation states (+1 and +2) both in solution and in solid. Among all bioactive metals, Cu exhibits by far the lowest concentration in cells (Andreini *et al.*, 2008). The extreme toxicity of elevated copper concentrations to all aquatic photosynthetic micro-organisms is usually explained to be due to blocking and reducing the thiol sites on proteins (e.g., Chang & Reinfelder, 2000). In particular, Cu^{2+} may bind to SH-group-containing glutathione (Kachur *et al.*, 1998), and phytochelatin production in algae is known to be induced by the presence of Cu in response to the toxicity of the metal (Le Faucher *et al.*, 2005; Le Faucheur *et al.*, 2006). The copper resistance systems of bacteria such as *Pseudomonas* involve the production of proteins that bind copper in the periplasm and close to the outer membrane (Cooksey, 1993, 1994). Because of the high Cu affinity to thiol groups of cell proteins such as glutathi-

one, no free copper is believed to occur in a bacterial cell (Rae *et al.*, 1999). Depending on anaerobic or aerobic conditions, different periplasmic regulator proteins control copper homeostasis, and the direct transport (efflux pump) of Cu^{+} from the periplasm to the outside may occur (see Nies, 2003 for a review). Most phototrophic micro-organisms exhibit strong demand for copper, because the efficiency of primary producers in the biosphere is reliant upon effective copper delivery to their thylakoids (Banci *et al.*, 2004). Cyanobacteria are the one bacterial group that have known enzymatic demand for cytoplasmic copper import (Tottey *et al.*, 2005) as Cu in a cyanobacteria is used as an enzymatic cofactor bound by S ligands. In contrast, anaerobic bacteria do not appear to use copper (Silver, 1997), although recent review of Cu-bearing proteins revealed that the only organisms that did not have Cu-handling capabilities are pathogenic and parasitic micro-organisms that obtained their Cu requirements from a host (Bertini *et al.*, 2010). Whether copper is taken up initially as Cu^{2+} and subsequently reduced to Cu^{+} or whether copper is reduced directly at the cell surface (before or concomitant with transport) is not fully established (Silver, 1997).

It is important to note that the copper sites in proteins have a higher affinity to Cu(I) than to Cu(II) (Silver, 1997; Huffman & O'Halloran, 2001); as a result, it can be hypothesized that the reduction of Cu(II) into Cu(I) may occur already at the cell interface although in situ spectroscopic evidences of this process are currently lacking. At the same time, both enzymatic and non-enzymatic reductions of Cu have been observed at cell surfaces, which may represent the initial step in the uptake of metal complexes (Jones *et al.*, 1987; Hassett & Kosman, 1995). In the simplest form of uptake by phytoplankton, metals are adsorbed onto sites in cell walls and cell membranes without being transported into cytoplasm (Hudson, 1998; Xue *et al.*, 1988). To address the first step of metal interaction with live cells, a significant amount of work has been devoted to copper binding to algal and bacterial surfaces using macroscopic techniques (Gonzales-Davila *et al.*, 1995; Gonzalez-Davila *et al.*, 2000; He & Tebo, 1998; Xue & Sigg, 1990). Nevertheless, provision of Cu limitation vs. toxicity for different aquatic micro-organisms remains largely unknown. This is partially because of the lack of studies dealing with in situ characterization of Cu chemical status in cells of micro-organisms. Among different *in situ* techniques, X-ray absorption spectroscopy (XAS) including the X-ray absorption near-edge structure region or XANES and the extended X-ray absorption fine structure region or EXAFS is the most powerful one enabling resolution, at the molecular scale, of the molecular environment of Cu both in inorganic (Fitts *et al.*, 1999; Peacock & Sherman, 2004; Furnare *et al.*, 2005) and in organic (Polette *et al.*, 2000; Kretschmer *et al.*, 2002; Strawn & Baker, 2008, 2009; Manceau & Matynia, 2010) matrices. In contrast to numerous works devoted to structural characterization of Cu associated with soil humic substances (Xia *et al.*, 1997; Karlsson *et al.*, 2006), plants (Merdy *et al.*, 2002; Parsons *et al.*, 2002; Tiemann *et al.*, 2002; Sahi *et al.*, 2007) and bacterial exopolysaccharides (Nagy & Szorcsik, 2002), only one study addressed Cu structural status in unicellular micro-organisms. Kretschmer *et al.* (2004) reported that during adsorption on freeze-dried cyanobacterium *Anabaena flos-aquae*, Cu(II) is coordinated exclusively by phosphate after adsorption at pH 2 and by carboxyl and amine ligands after adsorption at pH 5. In addition, significant proportion of Cu(I) coordinated to thiol and amine group was detected in whole-cell samples, which was absent in peptidoglycan fractions (Kretschmer *et al.*, 2004). Precise and quantitative characterization of copper speciation is important for predicting Cu toxicity for various aquatic micro-organisms, metal distribution coefficients between the cells and the environment, and Cu isotope fractionation induced by microbial activity.

This work is devoted to quantifying, using XAS, the main structural factors controlling Cu interaction with various aquatic micro-organisms, namely the nature and number of Cu-binding ligands, Cu-ligand interatomic distances and *in situ* redox state of Cu at the surface and inside the cells. This is the most straightforward and quantitative method for obtaining such in situ information on a metal in heterogeneous inorganic and biological samples (e.g., Banci *et al.*, 2004; Kelly *et al.*, 2008). However, the main weakness of XAS is that it requires, depending on the accuracy of structural parameters to be obtained, elevated metal concentrations in biological matrixes, typically 100's to 1000' ppm of metal in dry weight or 1–10 ppm of metal in solution interacting with biomass. Very often, such high concentrations of dissolved trace metal like Cu make the environmental relevance uncertain. A usual way to overcome this is to use high concentration of biomass to achieve the high ligand-to-metal ratio similar to that of natural settings. Another shortcoming of XAS is its statistical character making it difficult to detect a specific highly selective but low-abundance group ($<\sim$10%) in the overall spectrum reflecting the average metal status in the sample (e.g., Kelly *et al.*, 2008). While this feature reduces the efficiency of XAS in resolving metal toxicity vs. limitation to the micro-organisms, it is overwhelmed by (i) straightforward detection by XAS of the element's redox state, (ii) high precision in deriving first-shell metal–ligand interatomic distances (within 0.01–0.02 Å) and (iii) easy discrimination of light (e.g., O, N) vs. heavy (e.g., S) neighbors in the absorber's first atomic shell. This makes XAS the best method for characterizing the chemical status of the major and thus most geochemically important part of metal. This in turn provides straightforward constraints for interpreting metal isotopes fractionation because the latter is determined by the dominant chemical species of the metal (Navarrete *et al.*, 2011 and references therein). Taking into account the abovementioned specificity of XAS, we used this method for direct assessment of the dominant chemical

forms of Cu associated with various aquatic and soil micro-organisms.

Oxygenic (diatoms, cyanobacteria) and anoxygenic phototrophs were selected as three representative and contrasting taxons of photosynthesizing micro-organisms known to exhibit low tolerance to Cu. In addition, soil rhizospheric aerobic *Pseudomonas* grown in Cu-rich media were used as an example of heterotrophic, highly resistant to Cu microbes (Pokrovsky *et al.*, 2008a and references therein). Copper interaction with cell surface may occur via (i) reversible adsorption at the low-affinity, high-abundance surface sites (Gélabert *et al.*, 2006; Gonzalez *et al.*, 2010), (ii) strong binding with low-abundance specific sites of the cell surface (Gonzalez-Davila *et al.*, 2000), (iii) periplasmic complexation, reduction and storage (Beveridge, 1989; Navarrete *et al.*, 2011). The surface adsorption properties of these diverse micro-organisms at high Cu loading are mainly controlled by low-affinity carboxylate sites whose distribution and abundance at the cell surface were previously investigated using surface titration, electrophoresis, and surface adsorption techniques (Gélabert *et al.*, 2004; Pokrovsky *et al.*, 2008a,b; Gonzalez *et al.*, 2010). It can be expected that surface adsorption in Cu-sensitive (oxygenic photoautotrophs) and Cu-tolerant micro-organisms (soil heterotrophs) will occur in a similar manner, whereas the Cu assimilation will be different because of different detoxification mechanisms and different metal requirements of each representative species. This work is aimed at verifying this hypothesis via assessing the differences in the ligand identity and the redox status, coordination and first-neighbor distances of Cu adsorbed on and assimilated by micro-organisms.

MATERIALS AND METHODS

Micro-organism cultures

Freshwater diatoms *Navicula minima*, mesophilic cyanobacteria *Gloeocapsa* sp. f-6gl, anoxygenic photosynthetic purple bacteria *Rhodovulum steppense* A-20s, and soil aerobic gram-negative bacteria *Pseudomonas aureofaciens* CNMN PsB-03 were obtained from collections and cultured as described previously (Gélabert *et al.*, 2004; Pokrovsky *et al.*, 2008a,b; Gonzalez *et al.*, 2010; Bundeleva *et al.*, 2011). Purple bacteria were cultured anaerobically on Pfenning media with addition of 0.1 g L^{-1} of yeast extract and 2 g L^{-1} of acetate and pH = 7.4 (Pfennig & Trüper, 1989). Cyanobacteria *Gloeocapsa* sp. were cultured on EDTA-free D media (1) at pH = 8.0–8.2. Typical conditions of culture were the following: light intensity = 2–3 thousands lux, temperature = 28–30 °C, and stationary growth phase achieved after 1–2 weeks. The growth phase was assessed by measuring optical density or cell biomass vs. time.

The bacterial strain of soil aerobic gram-negative bacteria *P. aureofaciens* CNMN PsB-03 was isolated from soybean root-adhering (rhizospheric) soil for their capability of producing large amounts of gel-forming exopolysacharide (EPS) on a sucrose–peptone (SP) medium. Two samples of *P. aureofaciens* PsB-03 biomass were used in the present study. The first one consisted of cells growing in nutritive medium with sucrose and peptone (SP media), which yields an abundant EPS synthesis, and the second one contained cells growing in/on nutritive medium with succinic acid as the only carbon source (SA media), which results in very little EPS. The qualitative monosaccharide composition of the EPS produced in indicated media is different: the SP media yields the EPS composed of 76.1% fructose, and 11.4% glucose, whereas in the SA media, polysaccharides contain 49.9% of glucose, 22.3% of fructose, and 14% of mannose. Small amounts (<10% of total sugars) of rhamnose, ribose, xylose, and galactose were present in both EPS samples. Therefore, the most probable EPS for SP medium is the acidic polysaccharide levan (polyfructan). In contrast, glucan and some other heteropolymers are present in SA medium. Details of growth conditions, EPS characterization, and Cu binding to cell are given by Gonzalez *et al.* (2010).

Monospecific diatom cultures of freshwater periphytic *N. minima* (NMIN) were cultured to a concentration of $\sim 10^7$ cell L^{-1} at 20 °C in a sterile Dauta (freshwater) EDTA-free medium under continuous aeration at pH of 7.6–7.9 and $[Cu]_{tot} \sim 0.2$ μM (Gélabert *et al.*, 2004, 2007). Typical incubation time was 1–2 weeks. Diatoms were harvested from the late exponential to stationary growth phase and kept at 4 °C until use.

Copper incorporation in cells during microbial growth experiments was performed during 3–13 days at typical conditions of cell culturing. Copper was added in the EDTA-free nutrient media in the form of Cu sulfate or nitrate without any additional organic ligand. Total aqueous Cu^{2+} concentration ranged from 0.1 to 30 μM for cyanobacteria, from 6 to 15 μM for purple bacteria, and from 400 to 800 μM for heterotrophic rhizospheric bacteria. Other nutrient metals (Fe, Zn, Mn, Co, Ni, and Mo) were present in trace amounts requested for growth with concentrations of 1–2 orders of magnitude lower than that of copper. The main organic ligands controlling Cu speciation in diatoms and cyanobacteria growth media are cell exometabolites. For *Rhodovulum* sp. and *P. aureofaciens* growing in organic-rich nutrient media, in addition to cell exometabolites, soluble proteins, phosphate, and carboxylates are capable of complexing Cu in solution. We evaluated using Cu^{2+}-ion selective electrode (ISE) that more than 99% of total dissolved Cu at $[Cu^{2+}]_{tot}$ of 760 μM is complexed with phosphate and peptone in SP media (sample Ps-3) and with phosphate and succinate in SA media (sample Ps-5). The Pfenning media of *Rhodovulum* sp. complexed more than 90% of added Cu ($[Cu]_{tot}$ = 10 μM, sample Rh-3) as revealed by the ISE measurement because of the presence of yeast extract, phosphate, and malate. Unfortunately, the low resolution of Cu^{2+}-selective electrodes at Cu <1–10 μM and poor knowledge of Cu^{2+} complexes stability

constants with proteins and cell exometabolites did not allow precise reconstruction of free Cu^{2+} concentration in growth media. However, it is important to note that in all growth (incorporation) experiments in this work, the free Cu^{2+} ion concentration was 1–2 orders of magnitude lower than the total dissolved Cu concentration.

For all growth (incorporation) experiments, prior to the analysis, the cells collected via centrifugation were rinsed in dilute Cu-free $NaNO_3$ or NaCl aqueous solution and then in a 0.01 M EDTA solution for 10 min to remove Cu that was reversibly adsorbed on surface envelopes (e.g., Le Faucher *et al.*, 2005; Knauer *et al.*, 1997; Hudson & Morel, 1989). Routine optical examination of cell prior to the XAS experiments after EDTA washing did not reveal cell lysis and degradation. We also performed additional washing in inert electrolyte solution of the same ionic strength as growth media to insure complete removal of all the EDTA traces from the wet pellet. Note that depending on the duration of treatment and the concentration of complexant, it is difficult to differentiate between sorbed and assimilated or intracellular metal so that the lines between assimilation and incorporation into biomolecules and sorption to cell 'surfaces' are blurred. In this work, surface-adsorbed external (EDTA-removable) and incorporated (non-EDTA-removable) copper fractions are operationally defined entities (Ma *et al.*, 2003; De Schamphelaere *et al.*, 2005).

The biomass of live bacteria and diatom cell suspensions was quantified by measuring wet (centrifuged for 25 min at 4500 *g*) and dry (freeze-dried) weight. The conversion factors of wet to freeze-dried weight for studied micro-organisms were the following: *N. minima*, 10.0; *Rhodovulum* sp., 11.7; *Gloeocapsa* sp., 8.2; EPS-rich *P. aureofaciens*, 3.6; EPS-poor *P. aureofaciens*, 5.0. All adsortion and assimilation samples were prepared at the European Molecular Biology Laboratory (EMBL), freeze-dried and measured at the ESRF within several hours after the preparation.

Adsorption experiments, reversibility tests and chemical analyses

Copper adsorption experiments were designed to test the effect of solution pH and metal loading on chemical status of adsorbed Cu. For this, two types of experiments at 25 °C and 0.01 M $NaNO_3$ were performed: (i) adsorption at constant initial copper concentration in solution as a function of pH (pH-dependent adsorption edge) and (ii) adsorption at constant pH as a function of copper concentration in solution (adsorption isotherm). The range of adsorbed Cu concentration varied from 0.2 to 50 μmol/g_{wet} and the range of aqueous Cu concentration was between 0.1 and 300 μM. The latter values are significantly higher than those generally reported in natural settings (0.01–0.06 μM in rivers, Gaillardet *et al.*, 2003 and Pokrovsky *et al.*, 2010; 0.003–0.03 μM in lakes, Xue & Sigg, 1993; Shirokova *et al.*, 2010; 0.3–0.9 μM in groundwaters, Kharaka *et al.*, 1987). However, the biomass concentration used in experiments (1–10 g_{wet} L^{-1} or 0.1–1 g_{dry} L^{-1}) is several orders of magnitude higher than the bacterioplankton and phytoplankton concentration encountered in natural waters (typically 10–100 μg L^{-1}). As a result, the total ratio of metal to ligand used in our experiments is of the same order of magnitude as that in non-contaminated natural aquatic environments.

All experiments were performed in solutions at pH < 7 undersaturated with respect to secondary copper hydroxide or carbonate solid phases as verified by using the MINTEQA2 computer code and corresponding database (Allison *et al.*, 1991; Martell *et al.*, 1997). Before the adsorption experiment, the cells were rinsed first in 0.005 M Na_2H_2EDTA solution and then three times in 0.01 M or 0.1 M $NaNO_3$ solution using centrifugation at 4500 *g* (~500 mL of solution for 1 g of wet biomass) to remove, as possible, the adsorbed metals and cell exudates from the surface. Adsorption experiments were conducted at 25 ± 0.2 °C on continuously stirred suspensions of 0.01 M or 0.1 M $NaNO_3$ solution in 8-mL sterile polypropylene vials during 40 min–2 h. The biomass concentration was held constant at 4 or 10 g humid per L, and dissolved copper concentration in solution ($[Cu^{2+}]_{aq}$) spanned from 0.1 to 300 μM. Bacterial suspension was prepared first at circum-neutral pH of 5, and then pH of the solution was adjusted to the desired value using either NaOH or HNO_3. HEPES buffer, which is known not to complex divalent metals in aqueous solution (Mirimanoff & Wilkinson, 2000), was added to a concentration of 0.003 M to keep pH constant during adsorption isotherm measurements.

For all experiments, sterile de-ionized water (MilliQ, 18 MΩ) purged of CO_2 by N_2 bubbling was used. At the end of the experiment, the suspension was centrifuged and the resulting supernatant filtered through a 0.22-μm nylon filter, acidified with ultrapure nitric acid and stored in the refrigerator until analysis. The concentration of copper adsorbed to biomass in each vessel was calculated by subtracting the concentration of copper in the filtrate at the end of experiment from the initial concentration of metal added in the suspension. Blank experiments did not demonstrate, within the analytical uncertainty, Cu release into the solution from the original cells or Cu adsorption on reactor walls in the full range of pH (from 2 to 7). This also demonstrated the absence, within ±10% of total amount, of Cu oxy(hydr)oxides precipitation at the conditions where most of adsorption occurred (5 ≤ pH < 7). Exposure time varied from 0.5 min to 43 h to assess the kinetics of Cu adsorption process. For most experiments, exposure time was fixed to 2–3 h. Optical microscopic inspection of bacterial cells before and after adsorption experiments showed no visible change in the cell structure and shape. The cells remained intact and non-deformed, and no cell fragments could be detected.

The reversibility of Cu adsorption was first tested following the method developed by Fowle & Fein (2000). A

homogeneous parent suspension solution of bacteria + Cu + electrolyte was adjusted to pH ~7 at which 100% Cu was adsorbed onto microbial cells. After 3 h of adsorption contact time, aliquots of this parent suspension solution were taken and adjusted to sequentially lower pH values (from 6.9 to 2). The reaction vessels equilibrated at new pH values for 3 h were sampled for Cu. The concentration of desorbed copper in the supernatant allows calculation of the amount of irreversibly assimilated metal. This amount never exceeded 5–10%, suggesting an equilibrium adsorption process with negligible amount of copper penetrating inside the cell. The second reversibility test, used earlier for algae and bacteria (Slaveykova & Wilkinson, 2002; Smiejan *et al.*, 2003), consists of treating the cell suspension with 0.01 M EDTA solution at neutral pH during 2–3 min, separating the cells and the supernatant by centrifugation, filtration (<0.22 μm) and measuring dissolved copper concentration. The first method was tested for cyanobacteria and anoxygenic phototrophs, while the second method was employed for checking the reversibility of copper adsorption on soil bacteria *P. aureofaciens*. In all cases, good recovery (~95%) of adsorbed copper was achieved suggesting a truly reversible adsorption phenomenon.

All filtered solutions were analyzed for Cu ($[Cu]_{aq}$) using flame atomic absorption (AAS, Perkin Elmer 5100, HGA-600; Perkin Elmer, Norwalk, CT, USA) with an uncertainty of ±1% and a detection limit of 0.1 μM. For Cu concentration lower than 0.5 μμ, analyses were performed by ICP-MS (Perkin Elmer SCIEX, Elan 6000) with a detection limit of 1 nM and a precision of ±10% and 5% for 1–50 nM and 50–500 nM, respectively. Cu concentration in dry biomass was measured by AAS after its full acid digestion ($HNO_3 + H_2O_2$) performed in a clean room. Values of pH were measured using a Mettler Toledo® (Columbus, OH, USA) combined electrode, with an accuracy of ±0.02 units. Dissolved organic carbon (DOC) was analyzed using a carbon total analyzer (Shimadzu TOC-5000) with an uncertainty of 3% and a detection limit of 0.1 mg L^{-1}.

To account for the Cu(II) speciation in solution, *in situ* potentiometry was used to monitor the activity and free concentration of Cu^{2+} (aq) in cells suspension. Solid-contact Cu sulfide electrode (NIKO Analit®, Moscow, Russia) coupled with Ag/AgCl reference electrode in 3.5 M KCl connected with solution via 1 M $NaNO_3$ salt bridge was calibrated at $4 < pH < 6$ in standard $Cu(NO_3)_2$ solutions. Similar to previous works (i.e., Gélabert *et al.*, 2007; Gonzalez *et al.*, 2010), the electrode was fitted with a sterile dialysis membrane (Spectra Por® 6, 6–8 kDa, Spectrum Medical Industries, Los Angeles, CA, USA), which prevents fouling and oxidation of the ISE active surface by the bacterial cells and molecular oxygen, respectively. The membrane also prevented the biofouling of the electrode surface by large molecular size extracellular substances. The constant ionic strength of 0.1 M was maintained via addition of $NaNO_3$. Potentiometric measurements were performed at 25 ± 0.5 °C in the concentration range of 10^{-5} to 10^{-2} M with a detection limit of 10^{-6} M and an uncertainty of 5%; a Nernstian slope of 29.1 ± 0.5 mV/pCu was obtained. Before and after the measurements, the electrode was calibrated in cell supernatant solution having the same concentration of background electrolyte and bacterial exudates as the experimental solution.

All investigated samples are listed in Table 1. A novelty of our approach was that all samples for XAS analysis were prepared onsite at the European Molecular Biology Laboratory (EMBL) in the vicinity of the ESRF and processed at the beamline within several hours after the end of freeze-drying procedure. This greatly reduced the possibility of sample degradation and allowed achievement of the highest Cu concentration for XAS spectra acquisition without increasing the level of initial Cu loading. Note that freeze-dried and wet samples showed identical chemical status for studied other divalent metals such as Zn, in phytoplankton samples that appeared (Pokrovsky *et al.*, 2005). This is also consistent with results obtained by Sarret *et al.* (1998) who reported a minimal effect of freeze-drying on Zn and Pb speciation in organic material such as lichens.

XAS spectra acquisition and data analysis

X-ray absorption spectroscopy spectra (including XANES and EXAFS) of Cu-bearing solids, aqueous solutions, and freeze-dried cells were collected in transmission or fluorescence mode, depending on Cu concentration, at the Cu K-edge (~9.0 keV) over the energy range 8.7–9.9 keV on BM30b-FAME beamline at the European Synchrotron Radiation Facility. The energy was selected using a Si(220) double-crystal monochromator constantly calibrated using a 5-μm copper metal foil; its K-edge energy was set to 8.9785 keV at the first maximum of the first derivative of the spectrum. Harmonic rejection was archived with a rhodium-coated mirror. Spectra were collected at 5–10 K using a liquid-helium cryostat. The low temperature of acquisition is beneficial for (i) decreasing thermal disorder and thus improving significantly the signal-to-noise ratio and (ii) minimizing beam-induced damage in case of redox-sensitive elements like copper. Multiple scans of 40 min $scan^{-1}$ acquisition time were recorded at different spots of the sample to further avoid beam-induced reactions. Despite these precautions, some samples (e.g., Gl-series, Table 2) did exhibit progressive changes in XANES spectra upon beam exposure; thus, care was taken to exclude such affected scans from modeling. Different solid Cu(I) and Cu(II) organic and inorganic compounds and Cu(II) aqueous solutions were recorded in the same XAS session and served as standards of the local atomic environment of Cu in micro-organism samples (Fig. S1, Tables S1 and S2 of Data S1). Data analysis was performed with the HORAE package (Ravel & Newville, 2005) and following the recommendations of the International X-ray Absorption Society (IXAS, http://www.ixasportal.net/ixas/).

Table 1 Samples used for X-ray absorption spectroscopy measurements

Sample	Type of interaction	Medium, conditions	Duration of exposure	pH	$[Cu^{2+}]_{aq}$, μM (solution)	$[Cu]_{solid}$, $\mu mol/g_{dw}$
NMIN-1	Adsorption	0.01 M $NaNO_3$, light	40 min	6.0	0.9	17
Gl-1	Adsorption	0.01 M $NaNO_3$, dark	50 min	6.0	0.4	18
Gl-2	Adsorption	0.01 M $NaNO_3$, dark	50 min	4.0	20	31
Rh-1	Adsorption	0.1 M $NaNO_3$, light	1 h	5.5	22	38
Ps-1	Adsorption	0.1 M $NaNO_3$, light	2 h	5.8	28	123
Ps-2	Adsorption	0.1 M $NaNO_3$, light	2 h	2.2	28	38
Ps-4	Adsorption	0.1 M $NaNO_3$, light	2 h	5.8	12	25
NMIN-2	Incorporation	Dauta, light	76 h	7.8	0.1–0.2*	1.5
Gl-3	Incorporation	BG-11, no EDTA	7 days	8.5	30 ± 5	25
Rh-2	Incorporation	0.1 M $NaNO_3$, light	2 h	8.5	15†	38
Rh-3	Incorporation	Pfenning, light	13 days	8.5–9.2	10 ± 4*	38
Ps-3	Incorporation	SP media	3 days	6.9	765–115	31
Ps-5	Incorporation	SA media	3 days	7.1	765–415	31
Media-0	Complexation	Initial SP media	12 h	7.3	770	–
Media-1	Complexation	Cell supernatant	28 h	7.3	340	–

All samples were freeze-dried prior the analysis. NMIN = *Navicula minima*; Rh = *Rhodovulum* sp.; Gl = *Gloeocapsa* sp. f-6gl; Ps-1, 2, 3 = *Pseudomonas aureofaciens* grown in sucrose-peptone (SP) media, producing rich exopolysacharides (EPSs); Ps-4, 5 = *P. aureofaciens* grown in succinate media (SA), producing poor EPSs. Dissolved organic carbon concentration in all samples was below 10 mg L^{-1}. The ionic strength used in both adsorption and assimilation experiments of different micro-organisms was chosen to match the typical physiological (growth media) conditions. All solutions were undersaturated with respect to any individual solid phase of Cu. For Cu concentration in solution, *means that the value was maintained constant within ±10–20% (unless indicated) by adding fresh nutrient solution in the course of growth and †stands for the initial concentration in solution. The ranges of Cu concentration used for Ps-3 and Ps-5 samples reflect the uptake of Cu during cell growth. All growth (incorporation) samples were treated in EDTA after the experiment to remove surface-adsorbed metal. Intracellular incorporated or assimilated copper is conventionally defined as the fraction of total cell-bound metal, not extracted after 10–15 min treatment in 0.01 M EDTA solution at neutral pH.

Table 2 Structural parameters of the atomic environment of Cu adsorbed or incorporated by micro-organisms as derived from XANES and EXAFS spectra

Sample	$I_{edge\text{-}crest}$	$I_{8982-eV}$	% Cu(I)	Atom	*N*, atoms	*R*, Å	σ^2, $Å^2$	*R*-factor
Adsorbed Cu								
NMIN-1	1.12	0.43	40 ± 10	O/N	3.3 ± 0.8	1.98 ± 0.02	0.007 ± 0.003	0.030
Gl-1	1.10	0.48	45 ± 15	O/N	4.3 ± 0.5	1.99 ± 0.02	0.011 ± 0.003	0.011
Gl-2	1.12	0.39	30 ± 10	O/N	3.4 ± 0.5	1.97 ± 0.01	0.011 ± 0.003	0.012
Rh-1	1.09	0.57	50 ± 10	O/N	4.0 ± 0.5	1.96 ± 0.02	0.012 ± 0.004	0.030
Ps-1	1.27	0.31	20 ± 5	O/N	4.0 ± 0.5	1.95 ± 0.01	0.006 ± 0.002	0.016
Ps-2	1.05	0.59	60 ± 20	O/N	1.8 ± 0.5	1.96 ± 0.02	0.006 ± 0.002	0.016
				S	0.8 ± 0.3	2.29 ± 0.01	0.002 ± 0.001	
Ps-4	1.23	0.43	30 ± 10	O/N	3.0 ± 0.5	1.95 ± 0.02	0.006 ± 0.001	0.020
Incorporated Cu								
NMIN-2	1.18	0.30	30 ± 10	O/N	3.0 ± 0.5	1.95 ± 0.01	0.004 ± 0.001	0.010
Gl-3	1.31	0.13	≤10	O/N	3.2 ± 0.5	1.95 ± 0.01	0.003 ± 0.001	0.025
Rh-2	1.00	0.60	80 ± 10	O/N	2.0 ± 0.5	2.03 ± 0.02	0.008 ± 0.004	0.020
				S	1.5 ± 0.5	2.27 ± 0.01	0.008 ± 0.003	
Rh-3	1.01	0.55	85 ± 5	O/N	2.0 ± 1.0	2.10 ± 0.05	0.010 ± 0.005	0.020
				S	2.5 ± 0.5	2.32 ± 0.02	0.008 ± 0.003	
Ps-3	1.01	0.50	80 ± 5	O/N	2.0 ± 0.3	2.07 ± 0.05	0.009 ± 0.004	0.020
				S	2.0 ± 0.5	2.30 ± 0.02	0.010 ± 0.005	
Ps-5	1.28	0.20	20 ± 5	O/N	4.0 ± 0.5	1.96 ± 0.02	0.006 ± 0.001	0.013
Media-0	1.16	0.36	30 ± 10	O/N	3.5 ± 0.5	1.98 ± 0.02	0.009 ± 0.003	0.020
Media-1	1.20	0.29	20 ± 5	O/N	4.3 ± 0.7	1.99 ± 0.02	0.009 ± 0.002	0.010

Intensities of the 8982-eV feature and white-line (=max of the edge-crest amplitude) are relative to the absorption edge step of 1.00. Cu(I) percentage was estimated from linear combination fits using the set of Cu(I) and Cu(II) standard compounds (see Supplementary Information); the uncertainty stems mostly from the choice of the different standards with 2-, 3- or 4-coordinate Cu.

EXAFS fitted *k*- and *R*-ranges are 2.5–11.0 $Å^{-1}$ and 1.1–4.0 Å, respectively. *R* = copper-backscatterer mean distance, *N* = ligand coordination number, σ^2 = squared Debye-Waller factor (relative to $\sigma^2 = 0$ adopted in the calculation of reference amplitude and phase functions by FEFF); *R*-factor defines goodness of the total fit in *R*-space (Ravel & Newville, 2005). E°, the energy at which k = 0 when extracting the EXAFS signal, was set to 8990.0 eV for consistency; Δe, a non-structural parameter in EXAFS fit accounting for phase shift between experimental EXAFS spectrum and FEFF calculation, was found to be 3 ± 2 eV for all Cu-organic spectra.

Details of the reduction procedure can be found elsewhere (Pokrovski *et al.*, 2005; Pokrovsky *et al.*, 2005, 2008c; Borisova *et al.*, 2010). In addition, principal component analyses (PCA) of both XANES and EXAFS spectra of all microorganism samples were performed using the ITFA package (Rossberg *et al.*, 2003). These analyses identified at least five independent components necessary to describe the set of 15 XANES spectra suggesting variable and mixed Cu local coordination and molecular geometry depending on Cu redox state.

RESULTS

Adsorption of Cu on the cell surface

Macroscopic observations

Concentrations of adsorbed Cu ($[Cu]_{ads}$) as a function of equilibrium Cu concentration in solution ($[Cu^{2+}]_{aq}$) at pH 5–6 and pH-dependent adsorption edge for cyanobacteria, anoxygenic phototrophs, and soil *P. aureofaciens* are presented in Fig. 1. At constant pH, $[Cu]_{ads}$ is roughly proportional to $[Cu^{2+}]_{aq}$ over almost two orders of magnitude, with a constant slope close to 1, suggesting no change in the stoichiometry between Cu aqueous ions and the surface sites over the linear adsorption range (Fig. 1A). It can be seen in this figure that wet biomass normalized binding capacities of the three types of bacterial cells at pH between 5 and 6 are similar within the data scatter. At the same time, detailed analysis of adsorption curves demonstrates some variation of slopes in a concentration-dependent manner, which might reflect saturation of chemically different pools of ligands as follows from thermodynamics analysis of Cu adsorption on studied bacteria (Pokrovsky *et al.*, 2008a,b; Gonzalez *et al.*, 2010). In this study, the XAS data were collected in the region of metal and ligand concentration which was similar among all studied micro-organisms. As such, in the limited range of metal concentration, the various pools of surface ligands could not be rigorously tested.

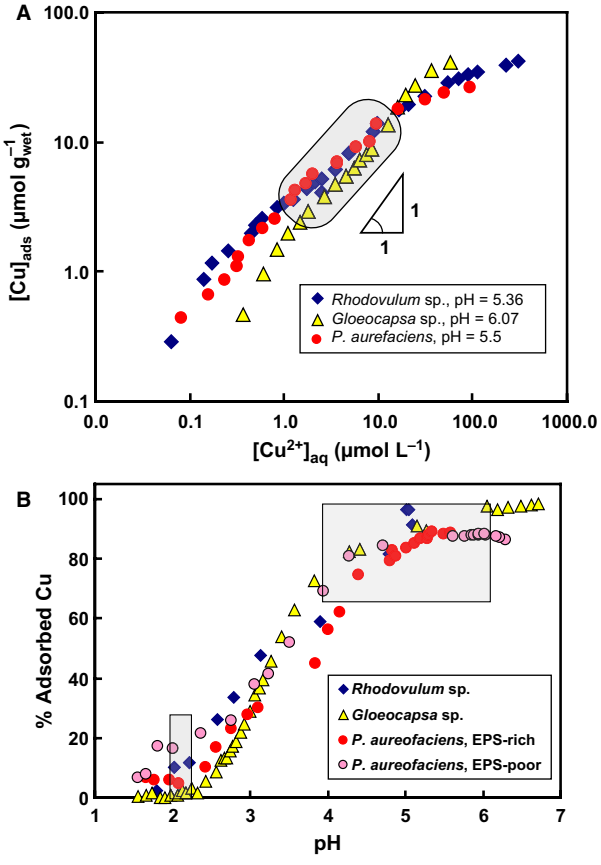

Fig. 1 (A) Concentration of adsorbed copper as a function of copper concentration in solution (constant-pH adsorption isotherm) for studied bacteria. Experimental conditions: 25 °C, pH 5.4–6.1, 4 g wet biomass per L, and 1 h of exposure time under darkness. The shaded area corresponds to the region of X-ray absorption spectroscopy (XAS) analysis. (B) Percentage of adsorbed Cu vs. pH for anoxygenic and oxygenic phototrophs, exopolysacharide (EPS)-rich and EPS-poor soil heterotrophs. Experimental conditions: $[Cu^{2+}]_o$ = 20 µM; 4 g_{wet} L^{-1}, 0.1 M $NaNO_3$. Shaded areas correspond to the regions of XAS analysis.

At constant biomass and total Cu concentrations, negligible adsorption is observed at pH < 2, an increase in adsorption occurs at 2 ≤ pH < 4 and 100% adsorption on the surface is achieved at pH > 5 (Fig. 1B). For pH-dependent adsorption edge, all the adsorption occurred at pH below 6 (Figs 1B and 3). At this pH, solution is strongly undersaturated ($\Omega < 10^{-2}$–10^{-3}) with respect to Cu hydroxides. Note that a pH-dependent adsorption edge is very similar among different microorganisms, in agreement with previous findings of 'universal' adsorption edge for other divalent metals such as Cd (Yee & Fein, 2001; Borrok *et al.*, 2004). Measurement of copper adsorption kinetics on *Rhodovulum* sp. and *P. aureofaciens* at pH 5–8.5 demonstrated that a majority of Cu is sorbed within 1–10 min (Fig. 2A,B, respectively). The adsorbed Cu concentrations do not differ between experiments of 1 and 24 h exposure time for *P. aureofaciens* (Fig. 3). For *Rhodovulum* sp. at $[Cu^{2+}]_{aq}$ > 1–10 µM, there was no difference in the proportion of adsorbed Cu after 1 and 18 h of exposure at pH of 7.1 (Fig. 4A). At lower Cu concentration, *Rhodovulum* sp. yielded smaller amounts of adsorbed Cu after 17 h of reaction under light compared to 1 h in-darkness exposure experiments at pH of 5.36 (Fig. 4B). This may suggest an active metabolic response to the presence of Cu, probably in the form of an efflux mechanism (e.g., Croteau *et al.*, 2004). Note that while the viability of *P. aureofaciens* was verified via routine culturing on agar plate and counting the live cell number, the metabolic activity of *Rhodovulum* sp. could not be tested.

General features of Cu K-edge XANES spectra of the biological samples

XANES Cu K-edge spectra of organic samples are rich in information and exhibit different features depending on the nature of ligands, Cu coordination, and oxidation state, as it

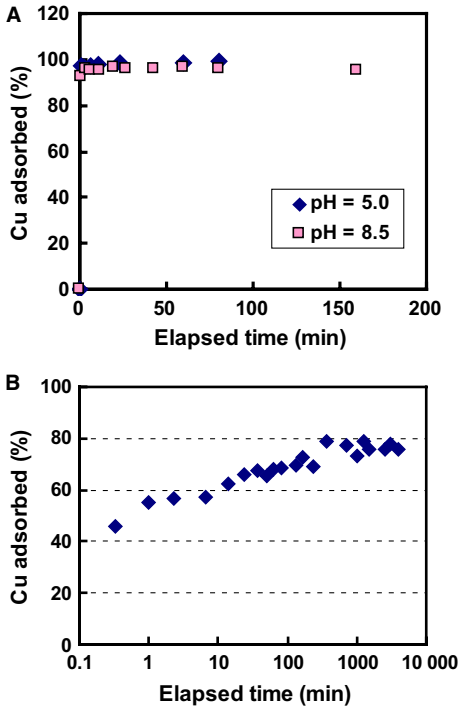

Fig. 2 Percentage of copper adsorbed on anoxygenic phototrophs *Rhodovulum* sp. A-20 s (A) and exopolysaccharide-rich soil heterotrophs *Pseudomonas aureofaciens* (B) as a function of elapsed time (min). Experimental conditions: 25 °C, 0.1 M $NaNO_3$, 4 g_{wet} L^{-1} biomass, pH = 5.0 and 8.5 (*Rhodovulum* sp.) and 5.85 (*P. aureofaciens*).

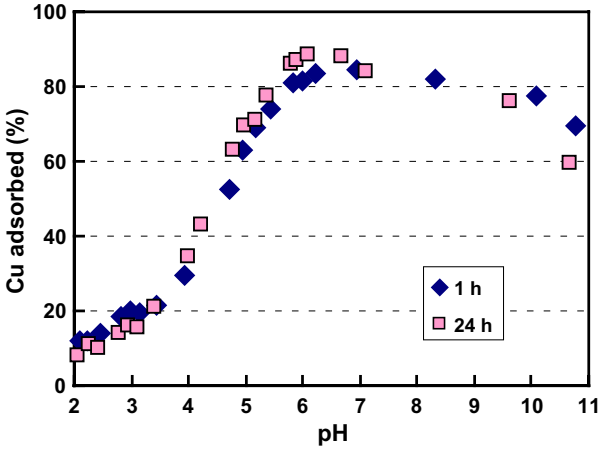

Fig. 3 Percentage of copper adsorbed on exopolysaccharide-rich *Pseudomonas aureofaciens* as a function of pH at different exposure times. Experimental conditions: 25 °C, 0.1 M $NaNO_3$, 4 g_{wet} L^{-1} biomass.

was demonstrated in the seminal paper of Kau *et al.* (1987) using a large database of Cu(I) and Cu(II)-bearing organic compounds. In particular, one characteristic feature of XANES spectra of most samples is the presence of a resonance at 8982.0 ± 0.5 eV with large variations of its amplitude depending on the sample (from 0.13 to 0.60 of the main-edge jump, Fig. 5, Table 2). This feature arises from the 1s-4p

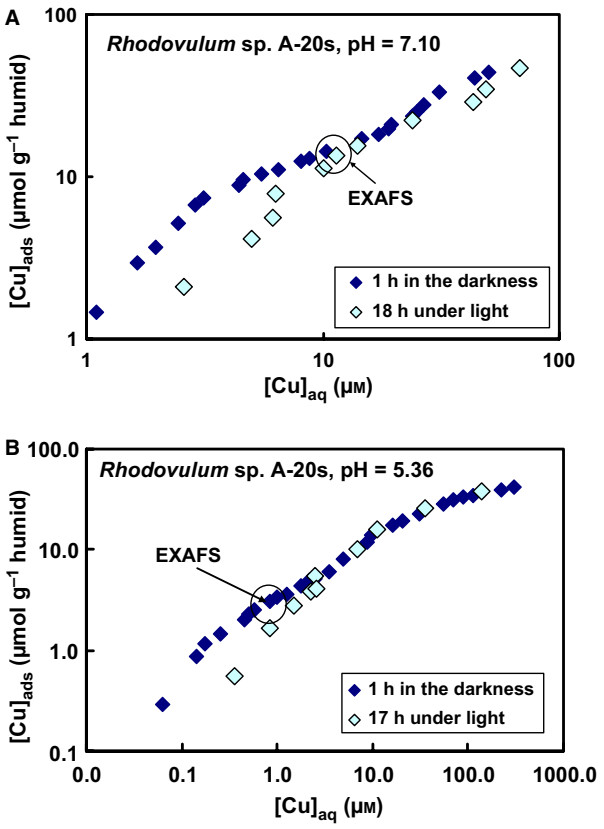

Fig. 4 Concentration of adsorbed copper as a function of copper concentration in solution (constant-pH adsorption isotherm) for *Rhodovulum* sp. at pH = 7.10 (A) and pH = 5.36 (B) after 1 and 17 h of exposure. Experimental conditions: 25 °C, 0.1 M $NaNO_3$, 4 g wet biomass/L. The encircled area corresponds to the samples for X-ray absorption spectroscopy measurements.

transition in Cu(I) and may be correlated with the ligand identity and site geometry of the cuprous ion (Kau *et al.*, 1987; Poger *et al.*, 2008; references therein). This feature is particularly pronounced in Cu(I)-O/Cl/S compounds in which Cu is linearly coordinated with two ligands of O (e.g., cuprite, Cu_2O), Cl (e.g., $CuCl_2^-$ aqueous complex), or S (e.g., $Cu(HS)_2^-$ aqueous complex, $(Et4N)_2Cu(SAd)_2$ compound where AdS is adamantine-2-thiolate), with amplitudes of 1.0 ± 0.1 of the main-edge jump as illustrated in the Electronic Supplementary Information 1 (Fig. S1, Tables S1 and S2 of Data S1). Tri-coordinated Cu(I) compounds exhibit much lower amplitudes for the 1s-4p resonance (typically 0.5–0.6 of the main-edge jump), whereas four-coordinated Cu(I) exhibits a 3-eV shift of this resonance to higher energies (Fig. S1 of Data S1). Thus, the 1s-4p transition may help to better understand the Cu(I) coordination in micro-organism samples. In contrast, the 8982-eV feature is not present in spectra of Cu(II) inorganic and organic solutions and O-bearing solids like CuO, $Cu(OH)_2$, and Cu(II)-phosphate, whose low-energy tail of the Cu K-edge edge has amplitudes <0.10 relative to the main absorption edge at this energy (Fig. S1, Tables S1 and S2 of Data S1). In copper sulfides like CuS and

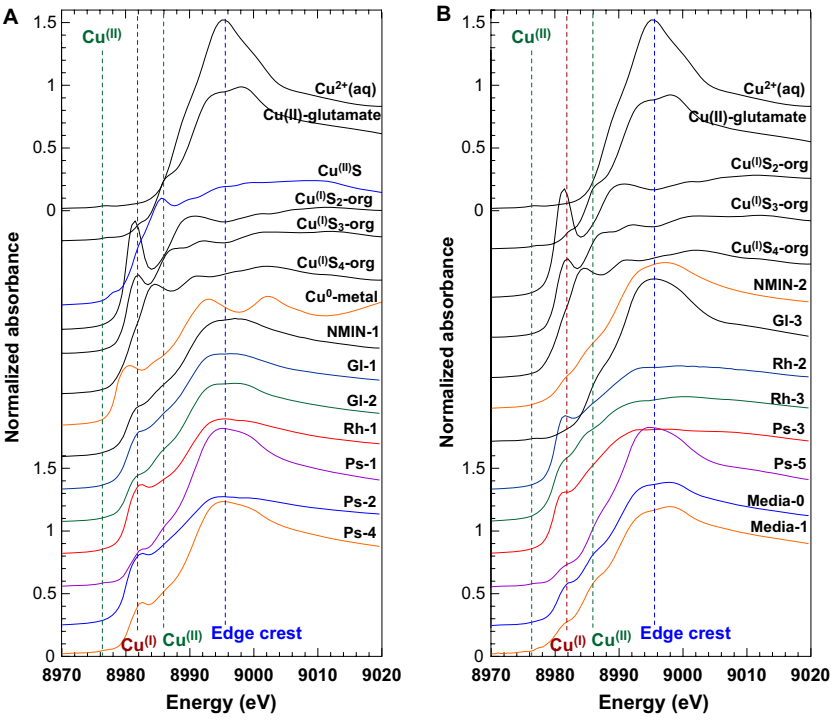

Fig. 5 Normalized K-edge XANES spectra of (A) adsorbed and (B) incorporated Cu micro-organism samples of this study (Table 2) and their comparison with pertinent reference compounds (see Data S2 for more reference spectra). The four vertical lines denote (in order of increasing energy, from left to right) the 1s-3d pre-edge Cu(II) transition at 8976 ± 2 eV, 1s-4p transition at 8982 ± 1 eV characteristic of Cu(I) compounds, the 8986–8988 feature typical of covalent Cu(II) complexes, and the main-edge-crest resonance particularly pronounced for Cu(II)-O/N complexes at ~8995 eV (see text for explanation). The following references are shown: Cu^0-metal = copper metal foil, $Cu^{(I)}S_4$-org = tetrahedral $Cu^I(C_5H_5NS_3)_2Cl_2$, Cu(I)S_3-org = trigonal $(Et_4N)_2Cu^I(SC_6H_4\text{-}p\text{-}Cl)_3$, Cu(I)$S_2$-org = linear $(Et_4N)Cu^I(SAd)_2$ where AdS^- is adamantine-2-thiolate (Poger *et al.*, 2008), $Cu^{(II)}S$ = tenorite mineral; $Cu^{(II)}$-glutamate = cupric glutamate aqueous solution, Cu^{2+} (aq) = cupric nitrate aqueous solution.

$CuFeS_2$, in which Cu is nominally divalent and coordinated with 3 or 4 sulfide ligands, and in most Cu(II) organic compounds with tri- and four-fold Cu coordination with S ± O/N ligands, this feature is not expressed explicitly either, representing the low-energy tail of the resonance at ~8986 eV typical of Cu(II) compounds with amplitudes ~0.5–0.6 at 8982 eV (Fig. S1, Table S2 of Data S1). Thus, Cu(II)-S bonds may be distinguished, at least qualitatively, from Cu(I)-S/N/O using the above features of XANES spectra.

The shape and amplitude of the 8982-eV feature of both adsorbed and incorporated Cu are not necessarily associated with the appearance of Cu-S bonds as found from EXAFS spectra, which allow robust detection of Cu-S first-shell contributions (sections 'XANES results of Cu adsorbed at the microorganism surface' and 'EXAFS features of intracellular copper'). It is thus very likely that significant part of Cu in samples exhibiting the 8982-eV resonance with amplitudes higher than ~0.3 is in the form of Cu(I) tri- or probably di-coordinated complexes with O(N) and/or S ligands. The amplitude of the 8982-eV feature in different samples is inversely correlated with that of the main K-edge resonance (around 8995 eV in most micro-organism samples of this study, Figs 5 and 6, Table 2) and, in some cases, with the average number of O/N neighbors in samples that show no detectable S in the first shell of Cu. Again, this is indicative of the presence of 2- and/or 3-coordinate Cu(I)-O/N complexes typical of the Cu^+ coordination chemistry, in contrast with Cu^{2+} that has a tendency to form 4-coordinate compounds with such ligands (Manceau & Matynia, 2010; Kau *et al.*, 1987). In addition, Cu(II)-dominated samples of micro-organisms and all reference Cu(II)-bearing solutions and solids, in which Cu is coordinated with O/N ligands, exhibit a small pre-edge at 8.877 ± 1 eV arising from the 1s-3d transition in Cu(II). Such a transition is forbidden in Cu(I) whose 3d electronic shell is filled ($3d^{10}$). Although this pre-edge feature is indicative of the presence of Cu(II), in most of our samples, it is obscured by the intense Cu(I) 8982-eV transition and/or Cu(II)-S low-energy tail, so that it could only be detected in few samples that show low fractions of Cu(I) (Ps-1, Gl-3, Ps-5, see below).

XANES results of Cu adsorbed at the micro-organism surface

Typical examples of scan evolution for *Gloeocapsa* sp. (Gl-1), *P. aureofaciens* (Ps-1, 3) and *Rhodovulum* sp. (Rh-1, 3) are presented in Data S2. In cyanobacteria (*Gloeocapsa* sp., Gl-1, Gl-2), the 8982-eV feature was found to grow with beam exposure, indicating that despite the cryogenic environment,

radiation-induced reduction (RIR) of Cu(II) could have been occurring in these samples. This is in agreement with reports of RIR phenomena for Cu in some soil bacteria samples (Strawn & Baker, 2009) and soil organic matter (Manceau & Matynia, 2010); consequently, the results of *Gloeocapsa sp.* should be interpreted with caution and thus only the least affected scans were considered in Table 2 and Fig. 5. In contrast, all other samples show almost no changes of the 8982-eV resonance and other XANES features upon beam exposure, suggesting that the presence of Cu(I) is intrinsic to these micro-organisms. Note also that none of the organic Cu(I) and Cu(II) standards measured in this study including aqueous solution of cell exometabolites show RIR effects.

XANES spectra of Cu adsorbed at the surface of oxygenic photoautotrophs (NMIN-1, Gl-1, Gl-2), rhizospheric *P. aureofaciens* (Ps-1, Ps-2, Ps-4), and anoxygenic phototrophs (Rh-1) show amplitudes of the 8982-eV feature between 0.3 and 0.6 of the edge jump (Table 2), demonstrating significant fractions of Cu(I) in these samples. In addition, the intensity of the main-edge crest is inversely proportional to that of the 8982-eV resonance. Because high main-edge intensities are typical of Cu(II)-O/N compounds (see section 'General features of Cu K-edge XANES spectra of the biological samples' and Fig. 6), their inverse correlation with the 8982-eV feature characteristic of Cu(I) is an independent confirmation of the reduction of a significant part of Cu(II) to Cu(I) upon sorption from aqueous solution onto micro-organism surfaces. The fractions of Cu(I) were estimated from linear combination fit (LCF) analyses of XANES spectra and using 19 reference organic and inorganic Cu(I)- and Cu(II)-bearing compounds and aqueous complexes with O, N, S, and Cl ligands from this study and published work (Kau *et al.*, 1987; Brugger *et al.*, 2007; Poger *et al.*, 2008; Etschmann *et al.*, 2010). The choice among the best corresponding standards for micro-organism spectra was performed using automated combinatorial fitting implemented in the Athena software from statistical analysis of all possible combinations of two, three, or four standards (Ravel & Newville, 2005). These analyses indicated that adsorbed Cu(II) is best represented by acetate, glutamate, or phosphate within statistical errors. Cu(I) in S-free samples is best fitted with linear or triangular Cu(I)-O/N coordination and with Cu(I)(S/Cl) standards (see Data S1) for samples that show Cu-S linkages according to EXAFS (see section 'EXAFS results and first neighbors of Cu adsorbed on the surface'). The derived Cu(I) fractions in oxygenic photoautotrophs (NMIN diatoms and Gl cyanobacteria samples) and anoxygenic phototrophs (Rh samples) are very similar, on average 40 ± 10% of total absorbed copper (Table 2); they exhibit larger variations, from 20% to 60% in rhizospheric bacteria (Ps samples). The largest fraction of Cu(I), 60 ± 10% (Table 2), is observed in EPS-rich soil heterotrophs (sample Ps-2 at acidic pH), the only one among the studied adsorbed Cu samples that shows the presence of sulfur atoms in the first Cu shell from EXAFS analyses (see next section).

The XANES spectra of most adsorption samples are thus supportive of the predominance of Cu(II)-O_4 and Cu(I)-(N_2/N_3) moieties common for Cu(II) and Cu(I) organic compounds, respectively (e.g., Kau *et al.*, 1987; Manceau & Matynia, 2010), with some contribution of Cu(I)-S_3 and/or Cu(I)-S_2 linkages in Ps samples for Cu adsorbed at acidic pH (Ps-2). Because of the similarly of the 8982-eV feature for Cu(I)-O/N/Cl/S environment of same geometry (2-, 3- or 4-coordinate), the quantification of Cu(I)-O/N vs. Cu(I)-S fractions is impossible in our samples based on XANES spectra only. In contrast, EXAFS spectra, fairly sensitive to the presence of heavier atoms (S) in the Cu coordination shell, allow independent quantification of the fraction of Cu-S linkages in such samples.

EXAFS results and first neighbors of Cu adsorbed on the surface

Modeling of EXAFS spectra of copper and other metals in natural organic and biologic matrixes is complicated by (i) distorted geometries and presence of different neighbors (O/N/S) in the metal nearest coordination shell, (ii) predominance in the next-nearest coordination shells of light atoms (C/O/N) exhibiting weak EXAFS signals, (iii) numerous multiple scattering paths in metal-organic ligand complexes, and (iv) multiple metal coordination environment and valence for the same ligand (e.g., $Cu^{II}S_4$ vs. $Cu^{I}S_2$). An additional limitation is the similarity of metal–ligand distances and coordination numbers for Cu(I) and Cu(II), which does not allow reliable deconvolution of the chemical status of each Cu redox form in micro-organism samples, even with accurate knowledge of the relative Cu(I)/Cu(II) content from XANES spectra (see previous section). The latter limitation is reflected by principal component analyses (PCA) of EXAFS spectra of both adsorbed and incorporated samples which demonstrate that only two independent factors are necessary for describing the set of 15 spectra within errors. These factors correspond to the two major Cu-O/N and Cu-S structural environments without distinction of the different Cu redox states and coordination geometries. In this study, we used the unique capacity of EXAFS analysis to quantify the two dominant Cu-O/N and Cu-S first-shell contributions based on their different metal-neighbor distances and O/N vs. S backscattering properties.

In samples of Cu adsorbed onto oxygenic photoautotrophs like diatoms and cyanobacteria (NMIN-1, Gl-1, Gl-2), and onto soil rhizospheric bacteria at pH = 5–6 (Ps-1, Ps-4), the Cu 1st shell EXAFS signal is dominated by 3–4 O/N atoms at 1.95–1.99 Å (Tables 2, S1 and S2 of Data S1). This is in agreement with both Cu^{2+}-$(O/N)_4$ planar ('equatorial') coordination and Cu-ligand distances in most Cu(II)-bearing solids, organic complexes, Cu adsorbed at the mineral surfaces and in aqueous solution (e.g., Peacock & Sherman, 2004;

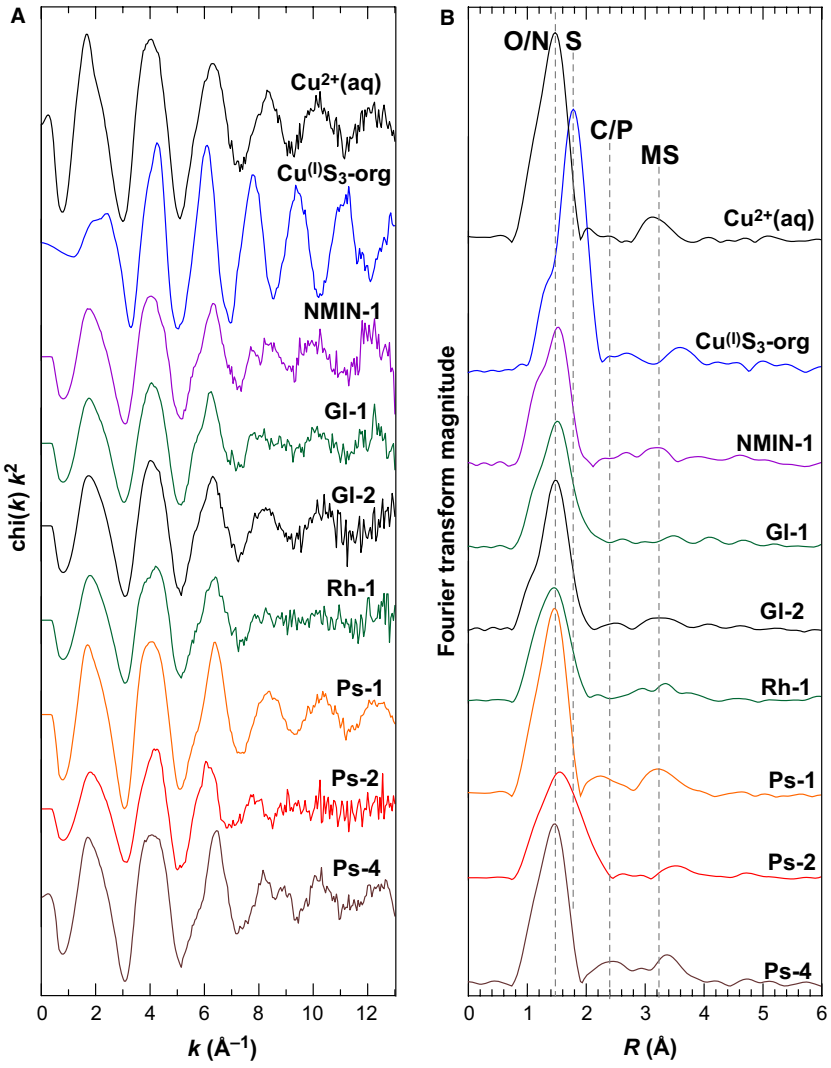

Fig. 6 (A) k^2-weighted EXAFS spectra of Cu adsorbed on the studied micro-organisms and (B) their corresponding Fourier transform magnitudes (not corrected for phase shift). (B) Vertical dashed lines on FT (B) denote the approximate positions (in order of increasing distance, from left to right) of first-shell O/N atoms, first-shell S atoms, possible next-nearest C/P atoms, and linear multiple scattering contributions (MS) arising from the square-like Cu(II)-$(O/N)_4$ cluster (see text). Also shown are two reference compounds, Cu^{2+} (aq) = copper nitrate aqueous solution and $Cu^{(I)}S_3$-org = $(Et_4N)_2Cu^I(SC_6H_4\text{-}p\text{-}Cl)_3$ solid, representing the two major Cu atomic environments in micro-organisms, Cu-O/N and Cu-S, respectively.

Pasquarello *et al.*, 2001; Alcacio *et al.*, 2001; Boudesocque *et al.*, 2004; Furnare *et al.*, 2005; Karlsson *et al.*, 2006) and Cu^+-$(O/N)_2$ or Cu^+-$(O/N)_3$ coordination environment known of Cu(I)-bearing organic compounds that show a large range of Cu-O/N distances (1.90–2.05 Å, Kau *et al.*, 1987; Poger *et al.*, 2008). The variations of EXAFS parameters within the equatorial O/N subshell of Cu(II) are too small to be correlated with bidentate vs. monodentate binding, Cu(II) fraction, or O vs. N ligands. Owing to the Jahn-Teller effect, the Cu^{2+} geometry in its O/N-bearing compounds is often regarded as pseudo-octahedral, with four equatorial strongly bounded (R_{O4} ~1.97 Å, Manceau & Matynia, 2010) and two axial ligands with much longer and looser bonds (R_{O2} ~2.2–2.6 Å, Kau *et al.*, 1987; Cheah *et al.*, 2000; references therein). Unambiguous detection of the latter by EXAFS is difficult. Attempts to include axial O atoms in the fits of micro-organisms and reference aqueous solutions yielded very weak EXAFS contributions having neither significant effect of the Cu-O/N equatorial parameters nor statistical fit improvement in most cases. In addition, these contributions are not expected for the Cu(I) coordination environments and they overlap with the much stronger Cu-S signal in Cu(I)-dominated S-bearing samples. Consequently, the axial Cu(II)-O/N bonds were neglected in EXAFS modeling of both adsorbed and incorporated samples.

For Cu adsorbed onto EPS-rich bacteria in acidic solution (Ps-2), EXAFS unambiguously detected the presence of sulfur in the first shell, which is found to be composed of

1.8 ± 0.5 O/N atoms at ~1.96 Å and ~0.8 ± 0.3 S atoms at ~2.29 Å (Table 2). The appearance of the Cu-S contribution is correlated with the high amplitude of the 8982-eV resonance in this sample ($I_{8982-eV}$ ~0.59), suggesting the formation of Cu(I)-S bonds of lengths typical for tri-coordinate Cu(I)-S_3 in many proteins (Cu-S distances are 2.26 ± 0.03 Å, Poger *et al.*, 2008). The fraction of Cu(I) bound to S estimated from the number of S atoms of EXAFS fits (0.8 ± 0.3) and assuming that all S is involved in Cu(I)-S_3 clusters is ~30% which is not enough to account for 60% of total Cu in the from of Cu(I) deduced from the XANES spectrum. This strongly suggests that half of Cu(I) in this sample is bound to N/O ligands. This non-sulfur environment is similar to that found for diatom and cyanobacteria adsorption samples showing no Cu-S linkages.

The outer shells of adsorbed Cu in studied micro-organisms cannot be resolved. We could not evidence clear contributions from atoms like C or P expected in the next-nearest shells of Cu(I) and Cu(II) in carboxyl or phosphoryl complexes typical of bacterial surface binding of most metals (Boyanov *et al.*, 2003; Pokrovsky *et al.*, 2005, 2008c). A weak contribution on the Fourier transforms of some low-Cu(I) samples (Ps-1, Ps-4) is apparent at ~3.2 Å (not corrected for phase shift, Fig. 6), which is because of linear multiple scattering events within the square Cu^{2+} $(O/N)_4$ clusters typical for Cu(II) compounds and aqueous solutions (Cheah *et al.*, 2000). Quantitative EXAFS modeling of this feature in our disordered organic samples is, however, complicated by additional contributions at similar distances arising from outer sphere water molecules and potentially numerous single and multiple scattering events within second- and third-shell C/P/O ligands typical of metal-organic complexes (e.g., Tella & Pokrovski, 2009). Analogous multiple scattering contributions from the linear Cu(I)-$(O/N/S/Cl)_2$ clusters are much weaker (e.g., Fulton *et al.*, 2000); they become almost negligible for non-linear geometries as shown by FEFF calculations. Thus, the weakening of this feature in Cu(I)-bearing samples (Ps-2, Rh-1, Gl-1; Fig. 6B) is an independent argument for the predominance of monovalent copper in the form of Cu-$(N/O/S)_3$ moieties, in agreement with LCA analyses of XANES spectra and EXAFS results for Cu 1st shell.

Chemical status of Cu assimilated by the micro-organisms

Effect of Cu on cell growth

Results of culture growth in the presence of Cu in solution are illustrated in Figs S1–S3 of Data S3 for oxygenic and anoxygenic phototrophs and EPS-rich, and EPS-poor soil heterotrophs, respectively. The effect of Cu on the cyanobacteria growth is already pronounced at $[Cu]_{tot}$ = 0.1–0.5 μM, and the growth is completely inhibited at $[Cu]_{tot} \geq 0.5$ μM. Anoxygenic phototrophs are less sensitive to micro-molar level Cu concentration as their growth is inhibited in the presence of >100 μM Cu. In contrast, growth of *P. aureofaciens* occurs at milli-molar level Cu concentrations and complete growth inhibition occurs at $[Cu]_{tot}$ > 1500 μM and 3000 μM for the EPS-poor and EPS-rich cultures, respectively. Note that reported copper concentrations represent the directly measured total dissolved (<0.22 μm) metal in solution. During growth of both photoautotrophs (pH = 7.5–8.5) and rhizospheric bacteria (pH = 5.2–6.5), more than 90% of Cu^{2+} in solution at the level of 1–10 μM of total Cu was complexed with organic ligands of the nutrient media (peptone of EPS-rich bacteria) or cell exometabolites (Cu^{2+}-free ion concentration ≤0.1 μM) as follows from *in situ* measurements with Cu^{2+}-selective electrode. Indeed, Cu complexation with organic ligands produced by green algae and diatoms and by siderophores from cyanobacteria is well established (McKnight & Morel, 1979, 1980; Ito & Butler, 2005).

XANES features of intracellular Cu

Normalized XANES spectra of incorporated Cu samples together with pertinent references are plotted in Fig. 5B. Similar to adsorbed Cu, most spectra are characterized by the 8982-eV feature whose intensity varies between 0.13 and 0.60 of the absorption edge (Table 2) and inversely correlates with the edge-crest amplitude around 8995 eV (Fig. 5B). Based on the correlations of Kau *et al.* (1987), combinatorial LCA of XANES spectra, and the results from EXAFS on the presence or not of S in the Cu 1st shell (see next section), it was found that Cu(I)-O/N two- and/or three-coordinate complexes account between 10% and 30% (±10%) of total intracellular Cu in diatoms (NMIN-2), cyanobacteria (Gl-3), EPS-poor *P. aureofaciens* (Ps-5), initial growth media (Media-0), and final *P. aureofaciens* cell supernatant solutions (Media-1). The major part of the incorporated Cu is likely to be in the form of Cu(II)-$(O/N)_4$ species similar to Cu(II) acetate or glutamate complexes. The fraction of Cu(I) in samples of anaerobic phototrophs *Rhodovulum* sp. (Rh-2, Rh-3) and EPS-rich *P. aureofaciens* (Ps-3) is much higher, around 80%, and is likely to be dominated by Cu(I)-S_3 geometries. These features are further supported by the independent EXAFS analysis.

EXAFS features of intracellular copper

In samples of Cu incorporated into oxygenic photoautotrophs like diatoms (NMIN-2) and cyanobacteria (Gl-3) and EPS-poor *P. aureofaciens* (Ps-5), the Cu 1st shell EXAFS signal is represented by 3–4 O/N atoms at 1.95–1.96 Å (Table 2), and no sulfur atoms are detected within the errors (N_S < 0.3). The outer-shell spectral features of these samples are characterized by pronounced multiple scattering signal from the planar square Cu(II)-$(O/N)_4$ cluster, in agreement with the dominant presence of Cu(II) as inferred from XANES spectra (Cu(II) fraction >70%, Table 2). Other next-nearest shell features, which may correspond to C/P atoms in Cu-O/N-C/P bonds, are too weak to be quantified. Their qualitative comparison with available Cu(II) reference compounds and

solutions (e.g., glutamate, oxalate, citrate, phosphate) does not reveal clear similarities. Tentatively, they might be attributed to 1–2 C or P atoms at 2.6–3.2 Å in the three samples (NMIN-2, Gl-3, and Ps-5), implying that incorporated Cu binds carboxylate or phosphoryl ligands, similarly to other intracellular metals (Pokrovsky *et al.*, 2005, 2008c).

In contrast, for Cu incorporated into anoxygenic phototrophs *Rhodovulum* sp. (Rh-3, Rh-2) and EPS-rich heterotrophs *Pseudomonas* (Ps-3), EXAFS analyses unambiguously detected the presence of ~2 sulfur atoms at ~2.30 Å, together with ~2 O/N atoms at 2.03–2.10 Å. The Cu-S and Cu-O/N distances are similar to those in proteins and other organic compounds containing tri- and four-coordinated Cu(I) and Cu(II) (e.g., Kau *et al.*, 1987; Pickering *et al.*, 1993; Pufahl *et al.*, 1997; Poger *et al.*, 2008). Although EXAFS is not capable of distinguishing Cu(I) from Cu(II) because of the similarity of their Cu-O/N and Cu-S bond lengths, LCA fits of XANES spectra of these samples yield ~80% of total copper as Cu(I). This compares favorably with the fraction of thiol complexes (X) derived from the number of S atoms from EXAFS spectra and assuming dominant Cu-S_3 stoichiometries ($X_{Cu(I)-S}$ = 100% × (2.0 ± 0.5)/3.0 = 70 ± 15%). Therefore, almost all incorporated Cu(I) in these samples is likely to be bound to thiol groups of intracellular proteins. The presence of next-nearest Cu atoms around the copper absorber in the form of Cu-S-Cu linkages with Cu-Cu distances of 2.7 ± 0.1 Å found in some proteins coordinating Cu in biological structures (Pickering *et al.*, 1993; Poger *et al.*, 2008) was not detected within the spectral statistics (≤~0.3 Cu atoms in the second shell) in *R. steppense* and *P. aureofaciens* (samples Rh-3 and Ps-3). It should be noted, however, that such linkages are often difficult to detect unambiguously even in a single-complex environment in isolated proteins owing to structural disorder caused by a large range of Cu-S distances and overlap in the EXAFS signal of Cu-Cu contributions with those of Cu-C from thiolate ligands (Pufahl *et al.*, 1997; Poger *et al.*, 2008).

EXAFS analysis of Cu chemical status in growth media of EPS-rich soil bacteria did not reveal significant differences between initial growth solution (Media-0) and cell supernatant solution collected after 28 h of growth at pH ~7 (Media-1). Both solutions show ~4 O/N atoms at ~1.99 Å (Table 2), together with the corresponding MS contributions at 3.2 Å (Fig. 7, not corrected for phase shift), similar to those in Cu(II)-$(O/N)_4$ reference aqueous solutions, whereas the next-nearest shell expected from Cu-O-C bonds at 2.6–3.3 Å is too weak to be quantified. This spectral pattern is in agreement with the dominant presence in these solutions of Cu^{2+} cation and/or Cu(II) bound to carboxyl or amide/amine ligands in a square planar geometry. Two important findings for the SP growth media are the following: (i) sulfur is not detectable in the Cu first shell and *ii*) the fraction of Cu(I) deduced from the 8982-eV (<20–30%) is smaller than that in intracellular assimilated samples (Ps-3).

DISCUSSION

Surface adsorption

Our XAS results show that upon short-term adsorption at the freshwater diatom and cyanobacteria cell surface from aqueous solution of inert electrolyte, Cu remains coordinated in the nearest shell with 3–4 oxygen atoms at 1.98 ± 0.01 Å likely in a pseudo-square geometry. Existing chemical and thermodynamic arguments suggest essentially carboxylate binding as follows from surface complexation modeling which is based on macroscopic adsorption experiments (cf. Pokrovsky *et al.*, 2008a,b; Gonzalez *et al.*, 2010). Reversible surface adsorption of copper at circum-neutral pH on anoxygenic phototrophs (sample Rh-1) and soil EPS-rich (sample Ps-1) and EPS-poor (sample Ps-4) bacteria yields essentially carboxylate environments, whereas the adsorption of Cu on EPS-rich soil bacteria in acidic solutions (Ps-2) brings about appearance of ~1 sulfur atom in the Cu first atomic shell. Sulfur-containing groups (-C-S- or -S-S-) in the EPS chains of rhizospheric bacteria of *Pseudomonas* genus were evidenced from macroscopic and spectroscopic observations (Emnova *et al.*, 2006, 2007). As a result, proteins and EPS may form stable complexes adjacent to the outer membrane and participate in reversible adsorption of Cu(II) from solution on the surface. This is especially pronounced for Cu adsorption from acidic solution (sample Ps-2, Table 2 and Fig. 6). At such elevated acidities, binding to fully protonated carboxylate groups should be less significant than at neutral pH, and Cu binding may also occur to ligands other than carboxylate, such as sulfhydryl moieties (Gardea-Torresdey *et al.*, 1990), which have a much higher affinity for both Cu(I) and Cu(II).

The sulfhydryl groups of proteins are also known to control reversible adsorption of Cd on *Bacillus subtilis* and *S. oneidensis* bacteria at low surface loadings (Mishra *et al.*, 2010), comparable with those investigated in this study. In the case of Cd-bacteria interaction, production of Cd-binding sulfhydryl groups at the cell surface may represent a component of toxicity response mechanism located either on the cell walls or within the cell, which may be initiated even by non-metabolizing cells (Mishra *et al.*, 2010). Recently, adsorption of Cu(II) on *B. subtilis* has been studied using EXAFS (Moon & Peacock, 2011). At very high Cu concentration in solid, from 0.13 to 0.66 weight %, only monodentate, inner-sphere, Cu-corboxylate complex has been identified.

Intracellular assimilation

Copper assimilated by oxygenic photoautotrophs (samples NMIN-2, Gl-3) revealed a coordination environment with 3.0 ± 0.5 O/N atoms at 1.95 ± 0.01 Å, thus indicating slight but detectable shortening (by 0.04 ± 0.01 Å) of the average first-neighbor distances upon incorporation of Cu inside the cells, in agreement with formation of stiffer and less disordered

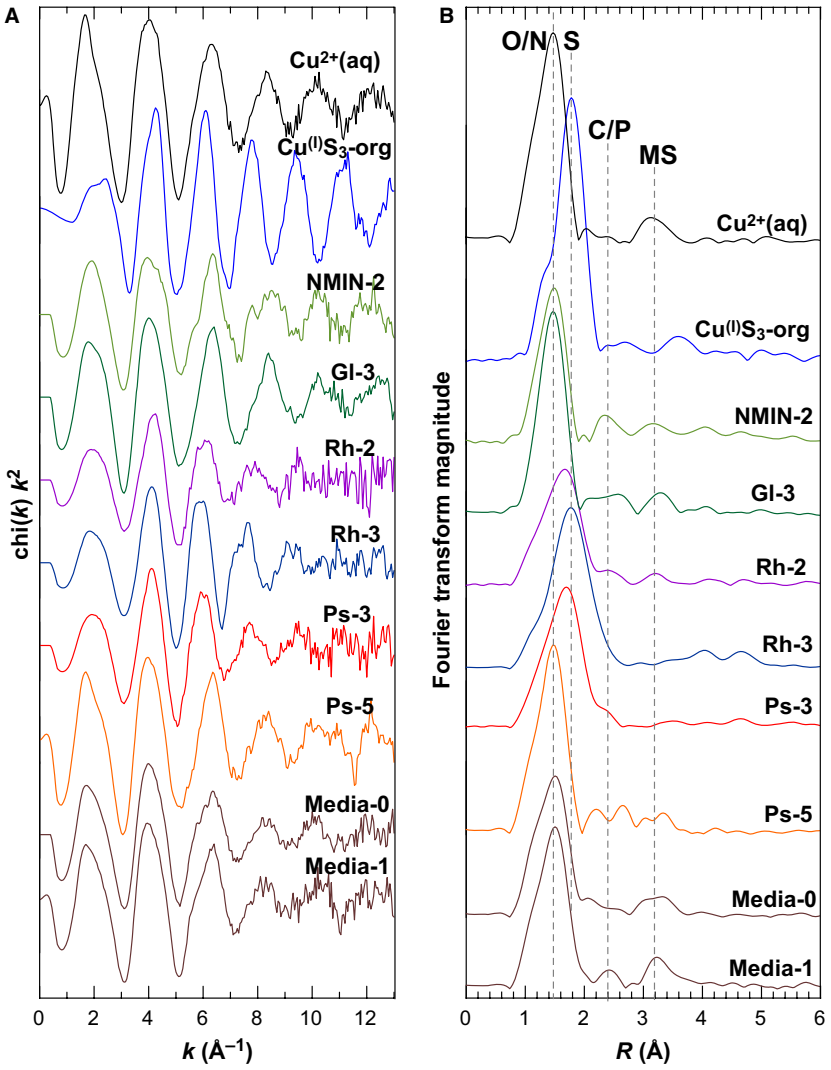

Fig. 7 (A) k^2-weighted EXAFS spectra of Cu incorporated in the studied micro-organisms and (B) their corresponding Fourier transform magnitudes (not corrected for phase shift). Vertical dashed lines on FT (B) denote the approximate positions (in order of increasing distance) of first-shell O/N atoms, first-shell S atoms, possible next-nearest C/P atoms, and linear multiple scattering contributions (MS) arising from the square-like [Cu(II)-$(O/N)_4$] cluster (see text). Also shown are two reference compounds, Cu^{2+} (aq) = copper nitrate aqueous solution and $Cu^{(I)}S_3$-org = $(Et_4N)_2Cu^I(SC_6H_4\text{-}p\text{-}Cl)_3$ solid, representing the two major Cu atomic environments in micro-organisms, Cu-O/N and Cu-S, respectively.

bonds compared with aqueous or surface Cu. The structural parameters of Cu binding to carboxylate groups of the studied micro-organisms are comparable with those available from the literature on Cu-organic matter interactions (Dupont *et al.*, 2002; Korshin *et al.*, 1998; Manceau & Matynia, 2010; Merdy *et al.*, 2002; Xia *et al.*, 1997). The presence of phosphoryl groups binding in incorporated or adsorbed copper by diatoms, cyanobacteria, and heterotrophic bacteria, as it was reported for other divalent metals such as Zn and Cd (Boyanov *et al.*, 2003; Guiné *et al.*, 2006; Mishra *et al.*, 2009; Ngwenya *et al.*, 2003; Pokrovsky *et al.*, 2005, 2008c), as well as Cu-phosphoryl binding with whole cyanobacteria in acidic solutions (Kretschmer *et al.*, 2004), cannot be either confirmed or ruled out within the uncertainty of our XAFS analysis.

In contrast to oxygenic photoautotrophs, irreversible assimilation of Cu by anoxygenic phototrophs (*Rhodovulum* sp. *A-20s*) during short-term exposure (sample Rh-2) and long-term growth (Rh-3) brings about the appearance of ~2 ± 0.5 sulfur atoms in Cu 1st coordination shell suggesting Cu scavenging in the form of both carboxylate/amine and sulfhydryl complexes. Note that unlike for adsorbed Cu for which macroscopic and thermodynamic arguments may be used to infer the predominant complex nature and stoichiometry, the assimilated metal may have carboxylate, phosphorylate, and amine-like environment (O, N as the first Cu neighbors and C, P as the second neighbors). Unambiguous identification of the second-neighbor chemical status of assimilated Cu(I, II) is not possible within the resolution of

the collected data and owing to the intrinsic limitations of XAS.

Similar to anoxygenic phototrophs, first-shell environment dominated by Cu-S complexes has been detected for Cu incorporated into soil aerobic bacteria (sample Ps-3). The average number of O/N and S neighbors, the absence of linear multiple scattering signal, and the fraction of Cu(I) deduced from XANES spectra all suggest the dominant presence of tri (and possibly four)-coordinate complexes in these samples, likely with histidine and sulfhydryl ligands in the same complex, rather than formation of linear S-Cu-S and N-Cu-N moieties.

As EXAFS did not detect sulfur atom in the first shell of aqueous Cu in the growth media solutions, either before or after cell cultivation in Cu-bearing solution (samples Media-0 and Media-1, Fig. 7), copper detoxification mechanisms are likely to be linked to inner cellular or subsurface enzymes or proteins. Therefore, the change of Cu speciation from carboxylate-dominated to thiolate-dominated occurs inside the cells of soil bacteria and not in the external media containing soluble EPS and cell exometabolites. It is known that in case of metal resistance mechanisms, bacteria of genera *Pseudomonas* are capable of accumulating Cu ions in the periplasm and outer membrane using the copper-binding cop proteins (Cooksey, 1994). Copper in the periplasm has been also observed in other gram-negative bacteria (Finney & O'Halloran, 2003; Bertini *et al.*, 2010; Navarrete *et al.*, 2011); for this reason, Cu associated with proteins (chaperones) in the periplasmic space is not as easily removed from the outer surface of the cells. As such, in contrast to adsorption phenomena, intracellular Cu uptake is likely to activate the detoxification mechanism via sulfhydryl group production, which occurs only above certain Cu concentration, specific to each micro-organism: 10–15 μM for anoxygenic phototrophs and 700 μM for soil heterotrophs. Despite the high toxicity of Cu to oxygenic photoautotrophs like cyanobacteria and diatoms, we did not observe any presence of sulfur in the first shell of Cu, likely because the concentration of free metal was too low to trigger active detoxification mechanisms.

The similarity of chemical status of intracellular Cu in cyanobacteria and freshwater diatoms, having different tolerance and requirement to Cu, is at first glance puzzling. However, our experiments were performed at rather high concentrations, when the passive rather than active defense (or uptake) mechanisms are pronounced. At these conditions, the proportion of Cu-sulfhydryl groups may be <10% of the total Cu, too low to be detected by EXAFS. It is possible that at lower Cu concentration in solution, the cells would preferentially accumulate this metal in the form of 'protein-active' sulfhydryl moieties and not dominantly carboxylate groups. Recent results on Cu status in photoautotrophs collected using ultra sensitive beamline supports this explanation (Pokrovsky *et al.*, 2011).

Cu(I) and comparison with literature data

A novel and unexpected feature of Cu interaction with anoxygenic phototrophs and soil heterotrophs, certainly linked to Cu binding to proteins, is the presence of monovalent Cu not only inside the cells as evidenced by XAS data of EDTA-treated, long-term Cu exposure samples (Rh-2, Rh-3) but also at the cell surface as it is seen from spectra of short-term surface-adsorbed Cu (samples Rh-1, Ps-2, Ps-4). We note that the highest fraction of Cu(I) is observed when S is present in the first atomic shell of adsorbed or incorporated Cu. This can be linked to a thiolate or cysteine environment of Cu(I) (Osman & Cavet, 2008). The Cu(I) signal is especially important in anoxygenic phototrophs cultured under anoxic conditions (samples Rh-2, 3). This corroborates previous reports of Cu(II) conversion into Cu(I) under anaerobic conditions of *E. coli* culturing (Beswick *et al.*, 1976). The presence inside cyanobacterial cells of metallothionein, a metal-binding protein, and other sulfhydryl and amine-containing proteins that bind Cu(I), was also reported by Kretschmer *et al.* (2004) and reviewed by Robinson *et al.* (2001). The finding of Cu(I) is in line with general knowledge of copper status in biological structures. Indeed, when the metal interacts with the cell surface, in addition to simple and reversible adsorption, it may undergo a chemical redox reaction (Price & Morel, 1990). For example, phytoplankton and yeast were reported to reduce Cu(II)-EDTA complexes to Cu(I) at their surfaces (Jones *et al.*, 1987; Hassett & Kosman, 1995). It is known that production of Cu(I) proteins of aerobic bacteria occurs mostly in the periplasm or outside the plasma membrane (Brown *et al.*, 1994). Therefore, appearance of Cu(I) in XANES spectra of Cu adsorbed on live (active) cell may indicate that some part of adsorbed ion is reduced and incorporated into protein trafficking machinery with Cu(I)-ligand complexes (Huffman & O'Halloran, 2001). Note that for other metals like Zn, up to 50% of the total metal amount stored in cells goes for transcription and translation machinery (Finney & O'Halloran, 2003). Cu(I) is often trigonally coordinated with two methionine and one histidine groups (Xue *et al.*, 2007). The Cu(I)-transporting protein of *B. subtilis* contains copper coordinated with three sulfur atoms, two of which are provided by the protein and one by dithiothreitol (Banci *et al.*, 2003). At the same time, we do not detect in any of studied micro-organisms Cu-O-Cu or Cu-S-Cu linkages like those reported in copper(I)-transporting proteins (Banci *et al.*, 2003). This led us to suggest that significant part of monovalent Cu is bound within the cell membrane, rather than with the intracellular proteins in cytoplasm. A schematic cartoon of Cu (II, I) interaction with the cell surface and redistribution within the cell compartments is given in Fig. 8. Adsorbed Cu(II) carboxylate/phosphoryl groups may facilitate intracellular Cu(II) storage, whereas Cu(II) reduction on the surface by membrane proteins is a prerequisite for Cu(I) transport and storage by sulfhydryl moieties of cell proteins.

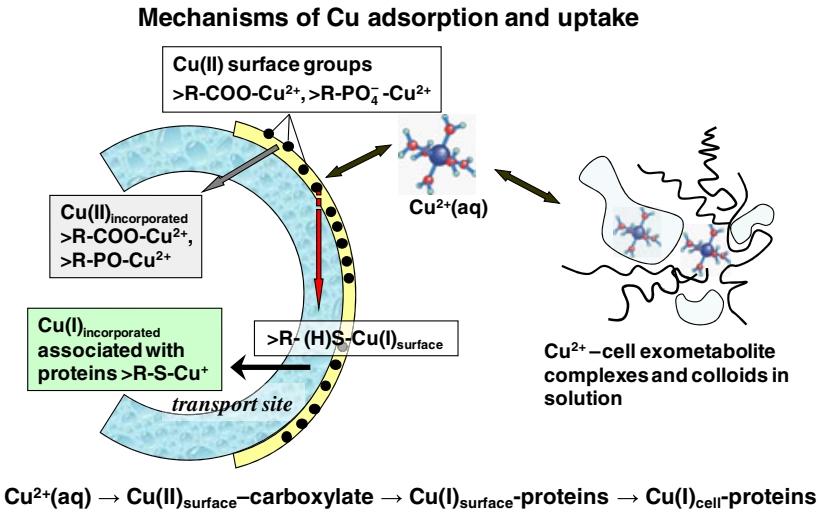

Fig. 8 Conceptual scheme of Cu interaction with studied micro-organisms. For oxygenic photoautotrophs, adsorbed Cu(II) carboxylate/phosphoryl groups may facilitate intracellular Cu(II) storage. For anoxygenic phototrophs and soil heterotrophs, the Cu(II) reduction on the surface by membrane proteins is a prerequisite for Cu(I) transport as sulfhydryl moieties of cell proteins.

Formation of Cu-thiol linkages stabilizes monovalent Cu at the bacterial surface; this stabilization is further pronounced for intracellular Cu. Each of described processes of Cu–ligand interaction and redox reactions is governed by (i) the nature of the micro-organism (aerobic vs. anaerobic, presence or not of the S-bearing EPS at the surface) and (ii) the total metal loading. In particular, at high copper concentrations in the system, the amount of available cell and membrane protein may be insufficient to convert all adsorbed Cu(II) into sulfhydryl Cu(I) and significant part of cell-associated Cu thus remains in the form of 'inert' Cu(II) carboxylates. In this regard, the concentration ratio of metal to the cell ligand, and not the value of the absolute metal concentration in solution, will define the molecular mechanism of Cu complexation and redox transformation.

Possible evolutionary implications

By encompassing a large variety of Earth's micro-organisms, from ancient anoxygenic phototrophic bacteria (APB) to modern freshwater diatoms, this work offers a new look at the copper–biota interaction in the context of life evolution on Earth. The largest proportion of Cu(I) linked to the presence of thiol groups occurs in anoxygenic phototrophs (purple bacteria). Although anoxygenic photosynthesis does not dominate primary production in the modern oceans, this metabolism may have been crucial for the growth of Archean and some Palaeoproterozoic stromatolites in shallow marine environments before the rise of oxygenic photosynthesis and the widespread atmospheric oxygenation (Olson & Blankenship, 2004; Canfield, 2005; Johnston *et al.*, 2009). Therefore, the dominance of Cu(I) in the cells of most primary photosynthetic organisms on Earth reflects the abundance of the metal's bioavailable forms, probably as Cu^{+} ions in the Archean ferric/ferro-sulfidic or Proterozoic sulfidic ocean. Among all bio-active metals (Fe, Ni, Co, Mn, Cu, Zn, and Cd), copper encountered the largest variations of its total concentration in the ocean since the Archean time (from 10^{-25} to 10^{-9} M, Saito *et al.*, 2003). These variations definitely stem from different redox states copper could have taken in surface waters during Earth's evolution. In neutral sulfide-bearing waters, solubility of Cu(I) sulfide (Cu_2S, chalcocite) is $\sim 10^5$ higher than that of Cu(II) sulfide (covellite). Therefore, in Precambrian sulfur-rich oxygen-poor ocean, Cu aqueous speciation was different from the present one and dominated by Cu(I) sulfide and Cu(I)-organic species. This would have required specific Cu(I)-acquisition mechanisms for micro-organisms inhabiting the Proterozoic and Archaean ocean. Such mechanisms were then inherited by APB cells. The late evolution of Cu- and Zn-binding structures (proteins) in micro-organisms (Dupont *et al.*, 2010) reflects the drastic change of oceanic geochemistry, marked by the Great Oxidation Event (e.g., Konhauser *et al.*, 2009) or a molecular adaptation specifically tied to eukaryotic evolution. Overall, there is a clear tendency of the decrease in both Cu(I) proportion and Cu-S linkages in the intracellular pool of Cu in the sequence APB $\rightarrow$ cyanobacteria $\cong$ diatoms which certainly reflects the trend of Cu speciation in the ocean and its bioavailability for aquatic organisms (e.g., Morel *et al.*, 2003). The fundamentally different ability to bind Cu in anoxygenic phototrophs relative to oxygenic photoautotrophs suggests that Cu concentration in solution may be among the controlling factors of their environmental niches. It follows that the two types of phototrophs could be separated by Cu chemocline in the paleo-ocean, suggesting a possible control of Cu spatial distribution on the global production of oxygen.

Concerning the status of copper associated with the latest among studied bacteria, aerobic heterotrophs, results of our study suggest that the surface proteins and EPS uptake by copper is the main factor defining the chemical status of Cu within these cells. Indeed, for the same bacterial species *P. aureofaciens,* only EPS-rich strain yielded S-bearing ligands and, consequently, high proportion of Cu(I) in the first atomic environment of copper (samples Ps-2, Ps-3, Table 2). The evolutionary meaning of this finding may be that the EPS production of bacteria in the biomats can certainly facilitate the uptake and preservation of Cu(I) ions. As such, massive EPS production by first heterotrophic bacteria but also by EPS-rich cyanobacteria (e.g., Braissant *et al.*, 2003; Dupraz *et al.*, 2009) could be compatible with the presence of Cu(I) in the environment. The EPS production can also witness the first cell resistance mechanism to increasing Cu concentration in the seawater during the change from Cu(I, II)-sulfidic fluids to Cu(II)-oxygenated environments. Furthermore, if we hypothesize that the presence of Cu(I) in the cells inherits the former reduced environment, this study would suggest that the first aerobic heterotrophic bacteria were most likely present as EPS-rich, periphytic (stromatolite-like, shallow-water) forms rather than planktonic cells inhabiting the water column.

CONCLUSIONS

Our findings demonstrate that despite the common opinion that copper is toxic for photosynthetic aquatic micro-organisms because of blocking the thiol sites of the proteins, at least 90% (resolution of XAS measurements) of Cu adsorbed on and incorporated into freshwater cyanobacteria and diatoms reside in the carboxylate-like environment similar to other divalent metals. In the wide range of metal/cell ratio encompassed in this study, it is not excluded, however, that 10% or less of total adsorbed Cu that is undetectable by EXAFS ($N_S \leq \sim 0.3$ atoms) could still be bound to thiol sites, blocking these sites and contributing to toxicity. Highly specific Cu binding in the form of sulfhydryl groups in APB and EPS-rich soil *P. aureofaciens*, and Cu(II) conversion into Cu(I) both at the cell surface and in the cell interior represent other new features, which should be intimately linked to the bioavailability of this metal in the context of phototrophs and heterotrophs evolution on the Earth.

ACKNOWLEDGMENTS

We are grateful to K. Konhauser, five anonymous reviewers of Geobiology, and three anonymous reviewers of Environmental Science and Technology for their extremely useful and constructive comments. This work was partially supported by the ANR RE-SYST and EC2CO Cytrix (INSU-CNRS) programs and grant of Russian Federation FCP 'Kadry' 2011-1.5-505-008: GK 1 4.740.11.0935. We thank the ESRF committee Surfaces & Interfaces for providing beam time and access to the synchrotron facility. We are grateful to J.-L. Hazemann and O. Proux for their assistance during the synchrotron measurements and to C. Den Auwer, D. Testemale, B. Etschmann, and J. Brugger for providing XANES spectra of some Cu reference compounds.

REFERENCES

Alcacio TE, Hesterberg D, Chou JW, Martin JD, Beauchemin S, Sayers DE (2001) Molecular scale characteristics of Cu(II) bonding in goethite-humate complexes. *Geochimica et Cosmochimica Acta* **65**, 1355–1366.

Allison JD, Brown DS, Novo-Gradac KJ (1991) MINTEQA2/PRODEFA2, A geochemical assessment model for environmental systems. Version 3.0 user's manual: U.S. EPA, Athens, GA, 106p.

Andreini C, Bertini I, Cavallaro G, Holliday GL, Thornton JM (2008) Metal ions in biological catalysis: from enzyme databases to general principles. *Journal of Biological Inorganic Chemistry* **13**, 1205–1218.

Banci L, Bertini I, Del Conte R, Mangani S, Meyer-Klaucke W (2003) X-ray absorption and NMR spectroscopic studies of CopZ, a copper chaperone in *Bacillus subtilis*: The coordination properties of the copper ion. *Biochemistry* **42**, 2467–2474.

Banci L, Bertini I, Ciofi-Baffoni S, Su XC, Borrely GPM, Robinson NJ (2004) Solution structure of a cyanobacterial metallochaperone. *Journal of Biological Chemistry* **279**, 27502–27510.

Bertini I, Cavallaro G, McGreevy KS (2010) Cellular copper management – a user's guide. *Coordination Chemistry Review* **254**, 506–524.

Beswick PH, Hall GH, Hook AJ, Little K, McBrien DCH, Lott KAK (1976) Copper toxicity: evidence for the conversion of cupric to cuprous copper in vivo under anaerobic conditions. *Chemico-Biological Interaction* **14**, 347–356.

Beveridge TJ (1989) Role of cellular design in bacterial metal accumulation and mineralization. *Annual Review of Microbiology* **43**, 147–171.

Borisova AY, Pokrovski GS, Pichavant M, Freydier R, Candaudap F (2010) Arsenic enrichment in hydrous peraluminous melts: insights from femtosecond laser ablation-inductively coupled plasma-quadrupole mass spectrometry, and in situ X-ray absorption fine structure spectroscopy. *American Mineralogist* **95**, 1095–1104.

Borrok D, Fein JB, Kulpa CF (2004) Proton and Cd adsorption onto natural bacterial consortia: testing universal adsorption behavior. *Geochimica et Cosmochimica Acta* **68**, 3231–3238.

Boudesocque S, Guillon E, Alpincourt M, Marceau E, Stievano L (2004) Sorption of Cu(II) onto vineyard soils: macroscopic and spectroscopic investigations. *Journal of Colloidal and Interface Science* **307**, 40–49.

Boyanov MI, Kelly SD, Kemner KM, Bunker BA, Fein JB, Fowle DA (2003) Adsorption of cadmium to *Bacillus subtilis* bacterial cell walls: a pH-dependent X-ray absorption fine structure spectroscopy study. *Geochimica et Cosmochimica Acta* **67**, 3299–3311.

Braissant O, Cailleau G, Dupraz C, Verrecchia AP (2003) Bacterially induced mineralization of calcium carbonate in terrestrial environments: the role of exo-polysaccharides and amino acids. *Journal of Sedimentary Research* **73**, 485–490.

Brown NL, Lee BTO, Silver S (1994) Copper: extracytoplasmic oxidases and matrix formation. In Metal Ions in Biological Systems, vol. 30, Book series, pp. 405–434.

Brugger J, Etschmann B, Liu W, Testemale D, Hazemann JL, Emerich H, Van Beek W, Proux O (2007) An XAS study of the structure

and thermodynamics of Cu(I) chloride complexes in brines up to high temperature (400 °C, 600 bar). *Geochimica et Cosmochimica Acta* **71**, 4920–4941.

Bundeleva IA, Shirokova LS, Bénézeth P, Pokrovsky OS, Kompantseva EI, Balor S (2011) Zeta potential of anoxygenic phototrophic bacteria and Ca adsorption at the cell surface: possible implications for cell protection from $CaCO_3$ precipitation in alkaline solutions. *Journal of Colloid and Interface Science* **360**, 100–109.

Canfield DE (2005) The early history of atmospheric oxygen: homage to Robert M. Garrels. *Annual Reviews in Earth and Planetary Science* **33**, 1–36.

Chang SIC, Reinfelder JR (2000) Bioaccumulation, subcellular distribution, and trophic transfer of copper in a coastal marine diatom. *Environmental Science and Technology* **34**, 4931–4935.

Cheah SF, Brown GE Jr, Parks GA (2000) XAFS study of Cu model compounds and Cu^{2+} sorption products on amorphous SiO^2, δ-Al_2O_3, and anatase. *American Mineralogist* **85**, 118–132.

Cooksey DA (1993) Copper uptake and resistance in bacteria. *Molecular Microbiology* **7**, 1–5.

Cooksey DA (1994) Molecular mechanisms of copper resistance and accumulation in bacteria. *FEMS Microbiological Reviews* **14**, 381–386.

Croteau MN, Luoma SN, Topping BR, Lopez CB (2004) Stable metal isotopes reveal copper accumulation and loss dynamics in the freshwater bivalve *Corbicula*. *Environmental Science and Technology* **38**, 5002–5009.

De Schamphelaere KAC, Stauber JL, Wilde KL, Arkich SJ, Brown PL, Franklin NM, Creighton NM, Janssen CR (2005) Towards a biotic ligand model for freshwater green algae: surface-bound and internal copper are better predictors of toxicity than free Cu^{2+}-ion activity when pH is varied. *Environmental Science and Technology* **39**, 2067–2072.

Dupont L, Guillon E, Bouanda J, Dumonceau J, Alpincourt M (2002) EXAFS and XANES studies of retention of copper and lead by a lignocellulosic biomaterial. *Environmental Science and Technology* **36**, 5062–5066.

Dupont CL, Butcher A, Valas RE, Bourne PE, Caetano-Anollés G (2010) History of biological metal utilization inferred through phylogenomic analysis of protein structures. *Proceedings of National Academy of Science USA* **107**, 10567–10572.

Dupraz C, Reid RP, Braissant O, Decho AW, Norman RS, Visscher PT (2009) Processes of carbonate precipitation in modern microbial mats. *Earth-Science Reviews* **96**, 141–162.

Emnova EE, Ciocarlan AG, Caunova NJ (2006) Exopolysaccharide synthesis of rhizospheric bacteria of *Pseudomonas* genus. *Ovidius University Annals of Chemistry* **17**(2), 187–189.

Emnova EE, Varbanets LD, Vasiliev VN, Ciocarlan AG, Brovarskaia OS, Caunova NJ, Ganea OG, Toma SI (2007) Properties of exopolysaccharides from rhizospheric fluorescent bacteria of *Pseudomonas* genus. *Bulletin of Moldovan Academy of Sciences. Life Sciences* **1**(310), 14–20.

Etschmann BE, Liu W, Testemale D, Müller H, Rae NA, Proux O, Hazemann JL, Brugger J (2010) An in situ XAS study of copper(I) transport as hydrosulfide complexes in hydrothermal solutions (25–592 °C, 180–600 bar): speciation and solubility in vapor and liquid phases. *Geochimica et Cosmochimica Acta* **74**, 4723–4739.

Finney LA, O'Halloran TV (2003) Transition metal speciation in the cell: insights from the chemistry of metal receptors. *Science* **300**, 931–936.

Fitts JP, Persson P, Brown GE, Parks GA (1999) Structure and bonding of Cu(II)-glutamate complexes at the γ-Al_2O_3-water interface. *Journal of Colloid and Interface Science* **220**, 133–147.

Fowle DA, Fein JB (2000) Experimental measurements of the reversibility of metal–bacteria adsorption reactions. *Chemical Geology* **168**, 27–36.

Fulton JL, Hoffmann MM, Darab JG (2000) An X-ray absorption fine structure study of copper(I) chloride coordination structure in water up to 325 °C. *Chemical and Physical Letters* **330**, 300–308.

Furnare LJ, Vailionis A, Strawn DG (2005) Polarized XANES and EXAFS spectroscopic investigation into copper(II) complexes on vermiculite. *Geochimica et Cosmochimica Acta* **69**, 5219–5231.

Gaillardet J, Viers J, Dupré B (2003) Treatise on geochemistry, 5 (eds. H.D. Holland and K.K. Turekian). In *Surface and Ground Water, Weathering, and Soils* (ed. Drever JI), Elsevier-Pergamon, Oxford, pp. 225–272.

Gardea-Torresdey JL, Becker-Hapak MK, Hosea JM, Darnall DW (1990) Effect of chemical modification of algal carboxyl groups on metal ion binding. *Environmental Science and Technology* **24**, 1372–1378.

Gélabert A, Pokrovsky OS, Schott J, Boudou A, Feurtet-Mazel A, Mielczarski J, Mielczarski E, Mesmer-Dudons N, Spalla O (2004) Study of diatoms/aqueous solution interface. I. Acid-base equilibria, surface charge and spectroscopic observation of two freshwater peryphytic and two marine planctonic diatoms. *Geochimica et Cosmochimica Acta* **68**, 4039–4058.

Gélabert A, Pokrovsky OS, Viers J, Schott J, Boudou A, Feurtet-Mazel A (2006) Interaction between zinc and freshwater and marine diatom species: surface complexation and Zn isotope fractionation. *Geochimica et Cosmochimica Acta* **70**, 839–857.

Gélabert A, Pokrovsky OS, Schott J, Boudou A, Feurtet-Mazel A (2007) Cadmium and lead interaction with diatom surfaces: a combined thermodynamic and kinetic approach. *Geochimica et Cosmochimica Acta* **71**, 3698–3716.

Gonzales-Davila M, Santana-Casiano JM, Perez-Pena J, Millero FJ (1995) Binding of Cu(II) to the surface and excudates of the alga *Dunaliela tertiolecta* in seawater. *Environmental Science and Technology* **29**, 289–301.

Gonzalez A, Shirokova LS, Pokrovsky OS, Emnova EE, Santana-Casiano JM, Gonzalez-Davila M, Pokrovski GS (2010) Adsorption of copper on *Pseudomonas aureofaciens*: protective role of surface exopolysaccharides. *Journal of Colloid and Interface Science* **350**, 305–314, doi.org/10.1016/j.jcis.2010.06.020.

Gonzalez-Davila M, Santana-Casiano JM, Laglera LM (2000) Copper adsorption in diatom cultures. *Marine Chemistry* **70**, 161–170.

Guiné V, Spadini L, Muris M, Sarret G, Delolme C, Gaudet J-P, Martins JMF (2006) Zinc sorption to cell wall components of three gram-negative bacteria: a combined titration, modeling and EXAFS study. *Environmental Science and Technology* **40**, 1806–1813.

Hassett R, Kosman DJ (1995) Evidence for Cu(II) reduction as a component uptake by *Saccharomyces cerevisiae*. *Journal of Biological Chemistry* **270**, 128–134.

He LM, Tebo BM (1998) Surface charge properties of and Cu(II) adsorption by spores of the marine *Bacillus* sp. Strain SG-1. *Applied and Environmental Microbiology* **64** 1123–1129.

Hudson RJM (1998) Which aqueous species control the rates of trace metal uptake by aquatic biota? Observations and predictions of non-equilibrium effects *Science of Total Environment* **219**, 95–115.

Hudson RJM, Morel FMM (1989) Distinguishing between extracellular and intracellular iron in marine phytoplankton. *Limnology and Oceanography* **34**, 1113–1120.

Huffman D, O'Halloran TV (2001) Function, structure and mechanism of intracellular copper trafficking proteins. *Annual Reviews in Biochemistry* **70**, 677–701.

Ito Y, Butler A (2005) Structure of synechobactins, new siderophores of the marine cyanobacterium *Synechococcus* sp. PCC 7002. *Limnology and Oceanography* **50**, 1918–1923.

Johnston DT, Wolfe-Simon F, Pearson A, Knoll AH (2009) Anoxygenic photosynthesis modulated proterozoic oxygen and sustained

Earth's middle age. *PNAS* **106**, 16925–16929, doi:10.1073/pnas.0909248106.
Jones GJ, Palenik BP, Morel FMM (1987) Trace metal reduction by phytoplankton: the role of plasmalemma redox enzymes. *Journal of Phycology* **23**, 237–244.
Kachur AV, Koch CJ, Biaglow JE (1998) Mechanism of copper-catalyzed oxidation of glutathione. *Free Radical Research* **28**, 259–269.
Karlsson T, Persson P, Skyllberg U (2006) Complexation of copper(II) in organic soils and in dissolved organic matter – EXAFS evidence for chelate ring structures. *Environmental Science and Technology* **40**, 2623–2628.
Kau LS, Spira-Solomon DJ, Penner-Hahn JE, Hodson KO, Solomon EI (1987) X-ray absorption edge determination of the oxidation state and coordination number of copper: application to the type 3 site in *Rhus vernicifera* laccase and its reaction with oxygen. *Journal of American Chemical Society* **109**, 6433–6442.
Kelly SD, Hesterberg D, Ravel B (2008) Analysis of soils and minerals using X-ray absorption spectroscopy. In: Methods of Soil Analyses. Part 5. Mineralogical Methods. SSSA Book Series, no. 5, chap. 14, pp. 387–464.
Kharaka YK, Maest AS, Carothers WW, Law LM, Lamothe PJ, Fries TL (1987) Geochemistry of metal-rich brines from central Missisippi Salt Dome Basin, USA. *Applied Geochemistry* **2**, 543–561.
Knauer K, Behra R, Sigg L (1997) Effects of free Cu^{2+} and Zn^{2+} ions on growth and metal accumulation in freshwater algae. *Environmental Toxicology and Chemistry* **16**, 220–229.
Konhauser KO, Pecoits E, Lalonde SV, Papineau D, Nisbet EG, Barley ME, Arndt NT, Zahnle K, Kamber BS (2009) Oceanic nickel depletion and a methanogen famine before the great oxidation event. *Nature* **458**, 750–754.
Korshin GV, Frenkel AI, Stern EA (1998) EXAFS study of the inner shell structure in copper(II) complexes with humic substances. *Environmental Science and Technology* **32**, 2699–2705.
Kretschmer XC, Gardea-Torresdey JL, Chianelli RR, Webb R (2002) Determination of copper binding in *Anabaena flos-aquae* purified cell walls and whole cells by X-ray absorption spectroscopy. *Microchemistry Journal* **71**, 295–304.
Kretschmer XC, Meitzner G, Gardea-Torresdey JL, Webb R (2004) Determination of Cu environments in the cyanobacterium *Anabaena flos-aquae* by X-Ray Absorption Spectroscopy. *Applied and Environmental Microbiology* **70**, 771–780.
Le Faucher S, Behra R, Sigg L (2005) Thiol and metal contents in periphyton exposed to elevated copper and zinc concentrations: a field and microcosm study. *Environmental Science and Technology* **39**, 8099–8107.
Le Faucheur S, Schildknecht F, Behra R, Sigg L (2006) Thiols in *Scenedesmus vacuolatus* upon exposure to metals and metalloids. *Aquatic Toxicology* **80**, 355–361.
Ma M, Zhu WZ, Wang ZJ, Witkamp GJ (2003) Accumulation, assimilation and growth inhibition of copper on freshwater alga (*Scenedesmus subspicatus* 86.81 SAG) in the presence of EDTA and fulvic acid. *Aquatic Toxicology* **63**, 221–228.
Manceau A, Matynia A (2010) The nature of Cu bonding to natural organic matter. *Geochimica et Cosmochimica Acta* **74**, 2556–2580.
Martell AE, Smith RM, Motekaitis RJ (1997) *NIST Critically Selected Stability Constants of Metal Complexes. Database Software Version 3.0*, Texas A & M University, College Station, TX.
McKnight DM, Morel FMM (1979) Release of weak and strong copper-complexing agents by algae. *Limnology and Oceanography* **24**, 823–837.
McKnight DM, Morel FMM (1980) Copper complexation by siderophores from filamentous blue-green algae. *Limnology and Oceanography* **25**, 62–71.
Merdy P, Guillon E, Dumonceau J, Alpincourt M (2002) Spectroscopic study of copper(II) – wheat straw cell wall residue surface complexes. *Environmental Science and Technology* **36**, 1728–1733.
Mirimanoff N, Wilkinson KJ (2000) Regulation of Zn accumulation by a freshwater gram-positive bacterium (*Rhodococcus opacus*). *Environmental Science and Technology* **34**, 616–622.
Mishra B, Boyanov MI, Bunker BA, Kelly SD, Kemner KM, Nerenberg R, Read-Daily BL, Fein JB (2009) An X-ray absorption spectroscopy study of Cd binding onto bacterial consortia. *Geochimica et Cosmochimica Acta* **73**, 4311–4325.
Mishra B, Boyanov MI, Bunker BA, Kelly SD, Kemner KM, Fein JB (2010) High- and low-affinity binding sites for Cd on the bacterial cell walls of *Bacillus subtilis* and *Shewanella oneidensis*. *Geochimica et Cosmochimica Acta* **74**, 4219–4233.
Moon EM, Peacock CL (2011) Adsorption of Cu(II) to *Bacillus subtilis*: a pH-dependent EXAFS and thermodynamic modeling study. *Geochimica et Cosmochimica Acta* **75**, 6705–6719.
Morel FMM, Milligan AJ, Saito MA (2003) Marine bioinorganic chemistry: the role of trace metals in the oceanic cycles of major nutrients. *Treatise on Geochemistry* **6**, pp.
Nagy L, Szorcsik A (2002) Equilibrium and structural studies on metal complexes of carbohydrates and their derivatives. *Journal of Inorganic Biochemistry* **89**, 1–12.
Navarrete JU, Borrok DM, Vivieros M, Ellzey JT (2011) Copper isotope fractionation during surface adsorption and intracellular incorporation by bacteria. *Geochimica et Cosmochimica Acta* **75**, 784–799.
Ngwenya BT, Suthermand IW, Kennedy L (2003) Comparison of the acid-base behaviour and metal adsorption characteristics of a gram-negative bacterium with other strains. *Applied Geochemistry* **18**, 527–538.
Nies DH (2003) Efflux-mediated heavy metal resistance in prokaryotes. *FEMS Microbiology Reviews* **27**, 313–339.
Olson JM, Blankenship RE (2004) Thinking about the evolution of photosynthesis. *Photosynthesis Research* **80**, 373–386.
Osman D, Cavet JS (2008) Copper homeostasis in bacteria. *Advanced and Applied Microbiology* **65**, 217–247.
Parsons JG, Hejazi M, Tiemann KJ, Henning J, Gardea-Torresdey JL (2002) An XAS study of the binding of copper(II), zinc(II), chromium(III) and chromium(VI) to hops biomass. *Microchemical Journal* **71**, 211–219.
Pasquarello A, Petri I, Salmon PS, Parisel O, Car R, Tóth E, Powell DH, Fischer HE, Helm L, Merbach AE (2001) First solvation shell of the Cu(II) aqua ion: evidence for fivefold coordination. *Science* **291**, 856–859.
Peacock CL, Sherman DM (2004) Copper(II) sorption onto goethite, hematite and lepidocrocite: a surface complexation model based on ab initio molecular geometries and EXAFS spectroscopy. *Geochimica et Cosmochimica Acta* **68**, 2623–2637.
Pfennig N, Trüper HG (1989) Anoxygenic phototrophic bacteria. In *Bergey's Manual of Systematic Bacteriology* (eds Boone DR, Castenholz RW, Garrity GM). Williams and Wilkins, Baltimore, MD, 3, pp. 1635–1709.
Pickering IJ, George GN, Dameron CT, Kurz B, Winge DR, Dance IG (1993) X-ray absorption spectroscopy of cuprous-thiolate clusters in proteins and model compounds. *Journal of American Chemical Society* **115**, 9498–9505.
Poger D, Fillaux C, Miras R, Crouzy S, Delange P, Mintz E, Den Auwer C, Ferrand M (2008) Interplay between glutathione, ATX1 and copper: X-ray absorption spectroscopy determination of Cu(I) environment in an Atx1 dimer. *Journal of Biological and Inorganic Chemistry* **13**, 1239–1248.

Pokrovski GS, Roux J, Hazemann JL, Testemale D (2005) An X-ray Absorption spectroscopy study of argutite solubility and germanium aqueous speciation in hydrothermal fluids to 500 °C and 400 bar. *Chemical Geology* **217**, 127–145.

Pokrovsky OS, Pokrovski GS, Gélabert A, Schott J, Boudou A (2005) Speciation of Zn associated with diatoms using X-ray absorption spectroscopy. *Environmental Science and Technology* **39**, 4490–4498.

Pokrovsky OS, Viers J, Emnova EE, Kompantseva EI, Freydier R (2008a) Copper isotope fractionation during its adsorption on soil and aquatic bacteria and metal hydroxides: possible structural control. *Geochimica et Cosmochimica Acta* **72**, 1742–1757.

Pokrovsky OS, Martinez R, Golubev SV, Kompantseva EI, Shirokova LS (2008b) Adsorption of metals and protons on *Gloeocapsa* sp. cyanobacteria: a surface speciation approach. *Applied Geochemistry* **23**, 2574–2588.

Pokrovsky OS, Pokrovski GS, Feurtet-Mazel A (2008c) A structural study of cadmium interaction with aquatic microorganisms. *Environmental Science and Technology* **42**, 5527–5533.

Pokrovsky OS, Viers J, Shirokova LS, Shevchenko VP, Filipov AS, Dupré B (2010) Dissolved, suspended, and colloidal fluxes of organic carbon, major and trace elements in the Severnaya Dvina River and its tributary. *Chemical Geology* **273**, 136–149.

Pokrovsky OS, Coutaud A, Pokrovski GS, Rols JL (2011) Structural study of copper chemical status adsorbed onto and incorporated by benthic algae and periphytic biofilm. *Mineralogical Magazine* **75**(3), 1654.

Polette LA, Gardea-Torresdey JL, Chianelli RR, George GN, Pickering I, Arenas J (2000) XAS and microscopy studies of the uptake and bio-transformation of copper in *Larrea tridentate* (creosote bush). *Microchemical Journal* **65**, 227–236.

Price NM, Morel FMM (1990) Role of extracellular enzymatic reactions in natural waters. In *Aquatic Chemical Kinetics: Reaction Rates of Processes in Natural Waters* (ed. Stumm W). Wiley, New York, pp. 236–258.

Pufahl RA, Singer CP, Peariso KL, Lin SJ, Schmidt PJ, Fahrni CJ, Cizewski CV, Penner-Hahn JE, O'Halloran TV (1997) Metal ion chaperone function of the soluble Cu(I) receptor Atx1. *Science* **278**, 853–856.

Rae TD, Schmidt PJ, Pufahl RA, Culotta VC, O'Halloran TV (1999) Undetectable intracellular free copper: the requirement of a copper chaperone for superoxide dismutase. *Science* **284**, 805–808.

Ravel B, Newville M (2005) ATHENA, ARTEMIS, HEPHAESTUS: data analysis for X-ray absorption spectroscopy using IFEFFIT. *Journal of Synchrotron Radiation* **12**, 537–541.

Robinson NJ, Whitehall SK, Cavet JS (2001) Microbial metallothioneins. *Advances in Microbiology and Physiology* **44**, 183–213.

Rossberg A, Reich T, Bernhard G (2003) Complexation of uranium(VI) with protocatechuic acid – application of iterative transformation factor analysis to EXAFS spectroscopy. *Analytical and Bioanalytical Chemistry* **376**, 631–638.

Sahi SV, Israr M, Srivastava AK, Gardea-Torresdey JL, Parsons JG (2007) Accumulation, speciation and cellular localization of copper in *Sesbania drummondii*. *Chemosphere* **67**, 2257–2266.

Saito MA, Sigman DM, Morel FMM (2003) The bioinorganic chemistry of the ancient ocean: the co-evolution of cyanobacterial metal requirements and biogeochemical cycles at the Archean-Proterozoic boundary? *Inorganica Chimica Acta* **356**, 308–318.

Sarret G, Manceau A, Cuny D, Van Haluwyn C, Déruelle S, Hazemann JL, Soldo Y, Eybert-Bérard L, Menthonnex JJ (1998) Mechanisms of lichen resistance to metallic pollution. *Environmental Science and Technology* **32**, 3325–3330.

Shirokova LS, Pokrovsky OS, Viers J, Dupré B (2010) Diurnal variations of trace elements and heterotrophic bacterioplankton concentration in a small boreal lake of the White Sea basin. *Annals of Limnology – International Journal of Limnology* **46**, 67–75, DOI: 10.1051/limn/2010011.

Silver S (1997) The bacterial view of the periodic table: specific functions for all elements. *Reviews in Mineralogy* **35**, 345–360.

Slaveykova VI, Wilkinson KJ (2002) Physicochemical aspects of lead bioaccumulation by *Chlorella vulgaris*. *Environmental Science and Technology* **36**, 969–975.

Smiejan A, Wilkinson KJ, Rossier C (2003) Cd bioaccumulation by a freshwater bacterium, *Rhodospirillum rubrum*. *Environmental Science and Technology* **37**, 701–706.

Strawn DG, Baker LL (2008) Speciation of Cu in a contaminated agricultural soil measured by XAFS, μ-XAFS and μ-XRF. *Environmental Science and Technology* **42**, 27–42.

Strawn DG, Baker LL (2009) Molecular characterization of copper in soils using X-ray absorption spectroscopy. *Environmental Pollution* **157**, 2813–2821.

Tella M, Pokrovski GS (2009) Antimony(III) complexing with O-bearing organic ligands in aqueous solution: an X-ray absorption fine structure spectroscopy and solubility study. *Geochimica et Cosmochimica Acta* **73**, 268–290.

Tiemann KJ, Rascon AE, Gamez G, Parsons JG, Baig T, Cano-Aguilera I, Gardea-Torresdey JL (2002) Heavy metal binding to inactivated tissues of *Solanum elaeagnifolium*: chemical and subsequent XAS studies. *Microchemical Journal* **71**, 133–141.

Tottey S, Harvie DR, Robinson NJ (2005) Understanding how cells allocate metals using sensors and metallochaperones. *Account in Chemical Research* **38**, 775–783.

Xia K, Bleam W, Helmke PA (1997) Studies of the nature of Cu^{2+} and Pb^{2+} binding sites in soil humic substances using X-ray absorption spectroscopy. *Geochimica et Cosmochimic Acta* **61**, 2211–2221.

Xue HB, Sigg L (1990) Binding of Cu(II) to algae in a metal buffer. *Water Research* **24**, 1129–1136.

Xue HB, Sigg L (1993) Free cupric ion concentration and Cu(II) speciation in a eutrophic lake. *Limnology and Oceanography* **38**, 1200–1213.

Xue HB, Stumm W, Sigg L (1988) The binding of heavy metals to algal surfaces. *Water Research* **22**, 917–926.

Xue Y, Davis AV, Balakrishnan G, Stasser JP, Staehlin BM, Focia P, Spiro TG, Penner-Hahn JE, O'Halloran TV (2007) Cu(I) recognition via cation-π and methionine interactions in CusF. *Nature Chemical Biology* **4**, 107–109.

Yee N, Fein J (2001) Cd adsorption onto bacterial surfaces: a universal adsorption edge? *Geochimica et Cosmochimica Acta* **65**, 2037–2042.

SUPPORTING INFORMATION

Additional Supporting Information may be found in the online version of this article:

Data S1 Structural data on Cu binding in reference compounds.

Data S2 Illustration of spectra evolution during synchrotron radiation experiments.

Data S3 Bacteria cell growth in the presence of Cu.

Please note: Wiley-Blackwell are not responsible for the content or functionality of any supporting materials supplied by the authors. Any queries (other than missing material) should be directed to the corresponding author for the article.